

Computational Study of Heat Exchange System Performance  
Enhancement using Nanofluids



By

HAFIZ AZEEM HAMZA

Fall 2019-MS CS&E 00000317558

Supervisor

DR. AMMAR MUSHTAQ

Department of Engineering

School of Interdisciplinary Engineering & Sciences (SINES)

National University of Sciences and Technology (NUST)

Islamabad, Pakistan

December 2022

Computational Study of Heat Exchange System Performance  
Enhancement using Nanofluids



By

HAFIZ AZEEM HAMZA

Fall 2019-MS CS&E 00000317558

Supervisor

DR. AMMAR MUSHTAQ

---

A thesis submitted in conformity with the requirements for  
the degree of *Master of Science* in  
Computational Science and Engineering

Department of Engineering  
School of Interdisciplinary Engineering & Sciences (SINES)  
National University of Sciences and Technology (NUST)

Islamabad, Pakistan

December 2022

## Declaration

I, *Hafiz Azeem Hamza* declare that this thesis titled “Computational Study of Heat Exchange System Performance Enhancement using Nanofluids” and the work presented in it are my own and has been generated by me as a result of my own original research.

I confirm that:

1. This work was done wholly or mainly while in candidature for a Master of Science degree at NUST
2. Where any part of this thesis has previously been submitted for a degree or any other qualification at NUST or any other institution, this has been clearly stated
3. Where I have consulted the published work of others, this is always clearly attributed
4. Where I have quoted from the work of others, the source is always given. With the exception of such quotations, this thesis is entirely my own work
5. I have acknowledged all main sources of help
6. Where the thesis is based on work done by myself jointly with others, I have made clear exactly what was done by others and what I have contributed myself

---

Hafiz Azeem Hamza

00000317558

## **Copyright Notice**

- Copyright in text of this thesis rests with the student author. Copies (by any process) either in full, or of extracts, may be made only in accordance with instructions given by the author and lodged in the Library of SINES, NUST. Details may be obtained by the Librarian. This page must form part of any such copies made. Further copies (by any process) may not be made without the permission (in writing) of the author.
- The ownership of any intellectual property rights which may be described in this thesis is vested in SINES, NUST, subject to any prior agreement to the contrary, and may not be made available for use by third parties without the written permission of SINES, which will prescribe the terms and conditions of any such agreement.

**I dedicated my work to my parents because I would not have been able to complete my studies without their prayers.**

## **Acknowledgments**

First and foremost, I want to express my gratitude to Allah Ta'ala for allowing my thesis to be finished and published. further thank to Allah for giving me the strength, courage, ability, and will to finish the thesis that satisfies my needs as well as those of my organization.

I would first want to express my gratitude to my research supervisor, Dr. Ammar Mushtaq (SINES, NUST), from whom I have gotten a great deal of support and assistance throughout my research. Every time I was in trouble or had a question concerning my research, Dr. Ammar's office door would always open for me. Dr. Ammar's expertise was really helpful to me as I developed my study topic and methodology. He provided me confidence and guided me in the correct direction whenever I was in trouble.

Additionally, I want to express my gratitude to my very dear friend Mr Altamash Shabir for his outstanding assistance and collaboration. He always had an answer when I was stuck on something. I wouldn't have been able to finish my thesis without his assistance. I am grateful for his assistance and patience throughout the entire thesis.

Finally, I would also like to special thank Dr. Junaid Ahmad Khan, Dr. Salma Sherbaz and Dr. Absaar ul Jabar for being on my Research guidance and evaluation committee.

# Table of Contents

<b>ABSTRACT</b> .....	11
<b>List of Figures</b> .....	12
<b>List of Tables</b> .....	13
<b>CHAPTER 1</b> .....	14
Introduction.....	14
1.1 Cooling System.....	14
1.2 Types of Cooling Systems.....	14
1.2.1 Air Cooling System.....	15
1.2.2 Water Cooling System .....	15
1.2.3 Radiator .....	17
1.2.4 Radiator Performance.....	19
1.3 Nanofluids .....	19
1.4 Literature Review.....	20
1.5 Research Gap .....	28
1.6 Objectives.....	28
<b>CHAPTER 2</b> .....	29
Computational Setup.....	29
2.1 Geometry.....	29
2.2 Computational Fluid Dynamics .....	30
2.2.1 Introduction to ANSYS Fluent.....	31
2.2.2 Pressure Based Solver .....	31
2.2.3 Discretization .....	32

2.2.4 Pressure Velocity Coupling.....	33
2.2.5 Boundary Conditions.....	34
2.2.6 Turbulence Model .....	35
2.2.7 Calculation of $Y^+$ .....	36
2.2.8 Computational Resources.....	36
2.3 Theory and Related Works.....	36
2.4 Validation with 2D Case .....	38
2.4.1 Grid Independence .....	38
2.4.2 Boundary Conditions.....	39
2.4.3 Simulations Results .....	40
2.5 Validation with 3D Case .....	43
2.5.1 Mesh of Radiator.....	43
2.5.2 Boundary Conditions.....	44
2.5.3 Simulations Results .....	45
<b>CHAPTER 3</b> .....	<b>46</b>
Simulations Results at Different Coolant Temperatures .....	46
3.1 Introduction .....	46
3.2 Boundary Conditions.....	46
3.3 Results .....	47
3.4 Concluding Remarks .....	50
<b>CHAPTER 4</b> .....	<b>51</b>
Simulations Results for Different Nanofluids .....	51
4.1 Introduction .....	51



4.2 Boundary Conditions.....	51
4.3 Contours Plots .....	51
4.4 Results by using <b>Al<sub>2</sub>O<sub>3</sub></b> Nanoparticles .....	52
4.5 Results by using <b>CuO</b> Nanoparticles .....	53
4.6 Concluding Remarks .....	56
<b>CHAPTER 5</b> .....	<b>57</b>
Summary and Future Recommendations .....	57
5.1 Summary .....	57
5.2 Future Recommendations.....	57
<b>REFERENCES</b> .....	<b>58</b>

## Nomenclature

$C_p$	Specific heat [J/kg K]	$Q$	Heat transfer [W]
$d$	Diameter [m]	$h$	Heat transfer coefficient [ $W/m^2K$ ]
$D$	Diameter of the tube [m]	$A$	Surface area [ $m^2$ ]
$K$	Thermal conductivity [W/m K]	$T_1$	Temperature of the wall [K]
$Nu$	Nusselt number	$T_2$	Temperature of air [K]
$Pr$	Prandtl number	$\dot{m}$	Mass flow rate [Kg/s]
$q''$	Heat flux [ $W/m^2$ ]		
$Re$	Reynolds number		
$T$	Temperature [K]		

## Greek letters

$\eta$	Viscosity (Pa .s)	$\rho$	Density [ $Kg/m^3$ ]
$\Phi$	Volume fraction	$\mu$	Dynamic viscosity [Kg/ms]

## Subscripts

bf	Base fluid
f	Fluid
H	Constant heat flux
In	Inlet
nf	Nanofluid
p	Particle
w	Wall

## ABSTRACT

In today's rapidly changing world, design engineers face challenges never encountered. With desires for higher efficiency at reduced size, operating machines at ideal conditions is a major bottleneck. Machines designed with such ambitious requirements produce immense heat. Therefore, the heat exchange system plays the most vital part for any machine to perform optimally. In order to maintain the ideal atmosphere, heat exchange systems are constantly operating with a failure possibility. The design of heat exchange systems has evolved throughout history to meet the necessities of that particular era. In the last few decades, the research community has focused on nanofluids and their contribution to maximizing the heat transfer rate compared to traditional coolants. Using nanoparticles in the base fluid as a coolant in automobile radiators is an essential topic for engine manufacturers due to the excellent enhancement in the cooling process. This research is undertaken to analyze the radiator performance and simulate the process using different coolant fluids. In the current work automobile radiator working principle was simulated, and the obtained results are in excellent agreement with the available literature for traditional coolants. The work was extended to perform a parametric study of adding nanoparticles into conventional coolants. The results of adding nanofluids in the engine radiator predicted that the heat transfer increased by increasing the volumetric concentration of nanoparticles in the base fluid. The outlet temperature of the coolant also increases by increasing the flow rate of the coolant. 8 percent volume fraction of  $Al_2O_3$  and  $CuO$  nanoparticles in base fluid results in maximum heat transfer, and hence minimum outlet temperature of the automobile radiator. The temperature reduction achieved with traditional coolant, water is 1.4% and improved to 1.74% and 1.9% for  $Al_2O_3$  and  $CuO$  at 4 L/min flow rate, respectively. Therefore,  $Al_2O_3$  and  $CuO$  based nanofluids are 24.9% and 36.7% more efficient than water.

## List of Figures

Figure 1.1 Pump forced cooling system. ....	16
Figure 1.2 3D model of radiator .....	17
Figure 1.3 Honey comb radiator [1] .....	18
Figure 1.4 Gilled tube radiator [2] .....	18
Figure 1.5 Tabular radiator [3].....	18
Figure 2.1 Radiator geometry .....	29
Figure 2.2 3D Rectangular tube of radiator .....	30
Figure 2.3 Mach number with flow regime .....	31
Figure 2.4 Schematic of 2D tube .....	38
Figure 2.5 Mesh I.....	38
Figure 2.6 Mesh II.....	39
Figure 2.7 Mesh III .....	39
Figure 2.8 Boundary conditions.....	40
Figure 2.9 Contours of static temperature.....	40
Figure 2.10 Heat transfer coefficient at different axial locations. ....	41
Figure 2.12 Structured grid of Radiator .....	44
Figure 2.13 Nusselt number calculation in fluent.....	45
Figure 2.14 Nusselt number comparison of CFD simulation with experimental results for pure water. ....	45
Figure 3.1 Contour plots of static temperature and velocity magnitude.....	47
Figure 3.2 (a) and (b) represent the outlet temperature w.r.t. Mass flow rate. (c) and (d) represents the outlet temperature w.r.t. Inlet temperature. ....	48
Figure 3.3 the temperature reduction of water at different inlet temperatures.	49
Figure 3.4 Heat transfer coefficient with flow rate of coolant.....	49

Figure 4.1 Contour plots of water and nanofluids. ....	51
Figure 4.2 Outlet temperature of water and mixture of water and <i>Al2O3</i> nanoparticles observed at different mass flow rates. ....	52
Figure 4.3 Outlet temperature water and mixture of water and <i>Cuo</i> nanoparticles observed at different mass flow rates. ....	53
Figure 4.4 A and B Temperature reduction of coolant at different flow rates.	54

### **List of Tables**

Table 2.1 Calculation for base fluid.....	31
Table 2.3 Size information of Mesh I.....	38
Table 2.4 Size information of Mesh II.....	39
Table 2.5 Size information of Mesh III .....	39
Table 2.6 Size information of radiator mesh. ....	44

### Introduction

Modern machines are designed with ambitious requirements of high efficiency and compact size produce immense heat. Therefore, heat exchange system plays the most vital part for any machine to perform optimally. To serve the ideal environment heat exchange systems are nonstop under threat of likely failures during process. The design of heat exchange systems has evolved throughout history to meet necessities of that particular era.

#### 1.1 Cooling System

Cooling system controls the automobile engine temperature. The following parameters have a direct impact on engine performance:

- i. The temperature of engine rises up to 1500 to 2000 °C due to the combustion of gasoline. The melting point of metals, that are used to make engines achieve at that temperature. Therefore, if the heat is not transfer to the atmosphere, it would affect the engine working.
- ii. At very high temperature, there is a chance of piston seizure

There are two main reasons to have an efficient cooling system:

- i. Cooling system must be capable of removing 30% heat that is generated during engine work. Too much removing of heat from system cause the inefficiency of combustion engine.
- ii. At the starting of engine, the temperature of engine is very low. So at the starting the cooling system should be very slow, because the engine parts achieve their optimum temperature to do work.

#### 1.2 Types of Cooling Systems

in many industrial, automobile application there are two main basic types of cooling system.

- i. Cooling system who uses air
- ii. Cooling system who uses water

### **1.2.1 Air Cooling System**

In air cooling system, the heat of the engine, that is conducted to the outer body of the engine, is removed away from the engine by the air. The air stream gets from the atmosphere. To increase the cooling by air, the fins are attached to the outer body of the engine to increase the surface area of engine body. During the manufacturing of cylinder, the fins are formed, basically the fins are metal surfaces. The following parameters have direct impact on the working of air-cooling system:

- i. The total surface area of fins
- ii. The velocity of cooling air
- iii. The amount of cooling air, that is bumping on the surface of engine
- iv. The temperature of cooling air

Air cooling system mostly use in small tractors (having less horsepower), small cars, motorcycles, small airplanes where the motions of the automobile gives very good velocity to air for cooling. The following are advantages of air cooled engines:

- i. The designs of air cooled engines are very simple
- ii. The weight of air cooled engine is light as compare to water cooled engine, due to the absence of water tank, water pump, cooling liquid weight, and radiator
- iii. Cost of air cooled engine is cheaper than water cooled
- iv. Less maintenance required for air cooled engines
- v. In air cooled engine there is no chance of corrosion, that's produce trouble for cooling liquid in radiator tubes

### **1.2.2 Water Cooling System**

In the working of automobile engines water cooling system has two purpose:

- i. It removes excessive amount of heat away from the engine and saves the engine from overheating

- ii. For economical and efficient working it stay the engine at optimum temperature

The water cooled system has two types:

- i. Non return/direct water cooled systems
- ii. Pump forced water cooled system

The **Non Return/Direct Water Cooled System** is suitable for large industries, and where the bulk of water is available for cooling. The water directly supplies from the water tank to engine where it absorbs heat from engine. The hot water is from the engine is not reuses and discharge from industry. Injection molding machines, tube well is an example of these systems.

The **Pump Forced Water Cooled System** is made with centrifugal pump that circulate the water from water tank to radiator, and the water flows from lower portion of the radiator to water tank through the water pump. These types of systems are used in trucks, cars, and tractors.

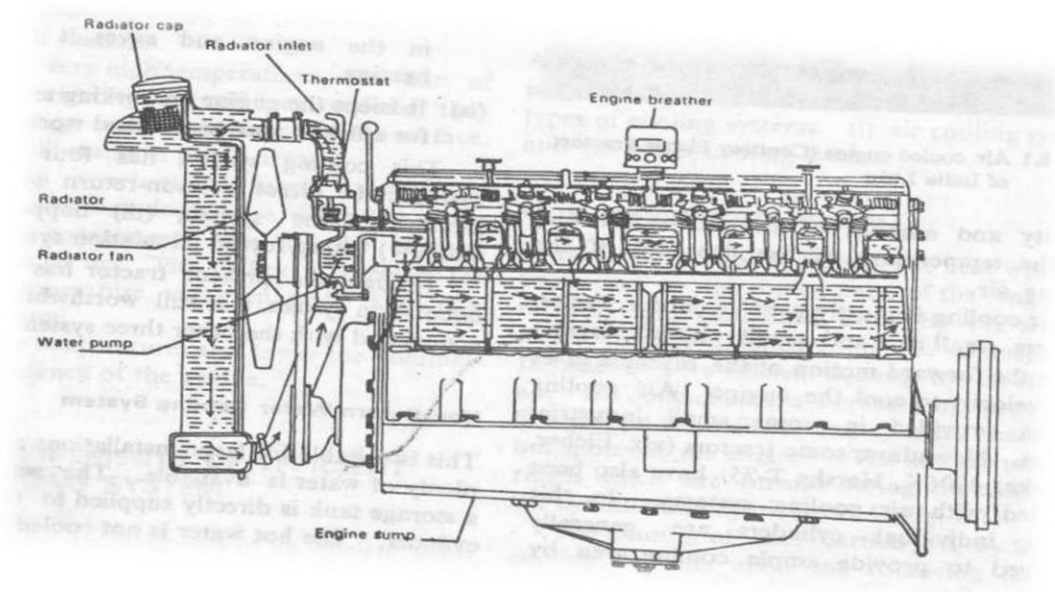


Figure 1.1 Pump forced cooling system.



The main parts of liquid/water cooling system are Hose pipes, Temperature gauge, Water jacket, Thermostat valve, Water pump, Radiator, Pressure cap, and Fan. The Fan has two purposes in the water cooling system:

- i. It throws the atmospheric air at radiator, to increase the heat transfer rate of a radiator
- ii. It throws the atmospheric air at the surface of the engine cylinder, and increase the heat transfer rate at outer surface of engine

### 1.2.3 Radiator

The basic purpose of a radiator is to cool the water that is coming from the engine. There are three main parts of radiator.

- i. Upper tank
- ii. Tubes/main core
- iii. Lower tank

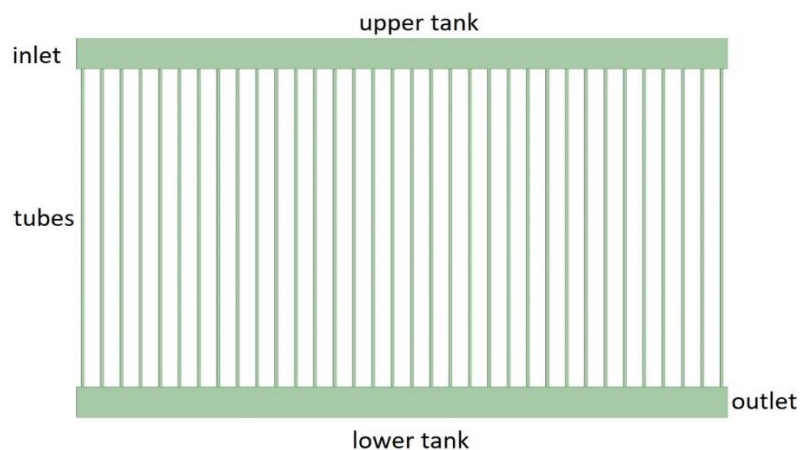


Figure 1.2 3D model of radiator

The radiators can be divided into three types; Honey comb radiator, Gilled tube radiator and Tabular radiator. Honey comb radiator consist of large number of air cells which are enclosed by water tubes. In this type of radiator, the block of any water passage affect the small part of radiator.

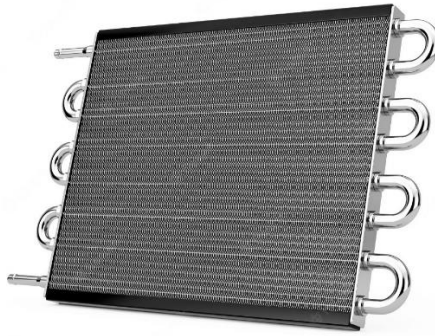


Figure 1.3 Honey comb radiator [1]

In Gilled Tube Radiator the water flows inside the main core. Each tube of the radiator consists of large number of fins that are connected to the outer surface of tube.



Figure 1.4 Gilled tube radiator [2]

Tabular Radiator is same as gilled tube radiator. In this type of radiator there is no unconnected fin for tubes. Tubes of the radiator fits in horizontal metallic sheet.



Figure 1.5 Tabular radiator [3]

### 1.2.4 Radiator Performance

Engine durability, reliability and maximum fuel efficiency achieved once it operates at optimum temperature. Therefore, the following parameters have direct impact on engine performance.

- i. Radiator size
- ii. Types of coolant
- iii. Coolant flow rate
- iv. Air temperature

There are many types of coolant that's are used in radiator. Water is the base coolant that is usually used in radiators. Another one is ethylene glycol used as a coolant in engines, the mixture of ethylene glycol and water using in car radiator as coolant. After the founding of nanofluids, scientists are working on the use of nanofluids in radiator.

Coolant flow rate is a basic parameter in heat transfer rate. From the literature it is observe that when the coolant flow rate increase the heat transfer rate is increase. So coolant flow rate is an important parameter for heat transfer coefficient.

Atmospheric air temperature has direct relation with heat transfer coefficient of an automobile radiator [4].

$$Q = hA(T_2 - T_1) \quad 1.1$$

### 1.3 Nanofluids

In improving the compactness and performance of applied engineering equipment's the low thermal properties of traditional coolant fluid has serious limitations. Nanofluids are a new world of nanotechnology. Nanofluids are heat transfer fluids, made by dispersing and suspending of nanoparticles in conventional heat transfer fluids. Nanoparticles diameter is in between 1-50 nm dispersed in base fluid (water) called nanofluids. In the past few decades, engineers and scientists have made remarkable discoveries in the field of nanotechnology. At a very low concentration of nanoparticles (less than 1 vol%)

can provide reasonable enhancement of thermal properties of base fluid. Some nanofluids provide high thermal properties such as high thermal conductivity at low volume fraction of nanoparticles. We can apply these discoveries in the field of medical and engineering applications. As a result, we can say that nanofluids technology emerged as a new area of science and engineering applications. Hence, nanofluids is a new field of research in applied sciences [5].

We can use nanofluids as a smart liquid, where heat transfer rate can be enhanced or reduced as per requirement [6]. In 2008 Routbort et al. started a project that used nanofluids for industrial applications. In the results they achieved good energy savings. The replacement of nanofluids with conventional coolant had save 1 trillion BTU of energy for U.S industry [7]. For cooling of microchips of electronic systems, nanofluids are used. The electronic application which we use fluids to control the heat nanofluids are also used. It is possible that, in the future, computer microchips will produce heat flux  $10 \frac{MW}{m^2}$ . we will use nanofluids to remove heat flux from computer microchips [8-9]. For the cooling of engine oil, engine cylinder conventional coolant has low thermal conductivity. To increase the heat transfer rate in the radiator of an automobile we will use nanofluids. In this research I will work on heat transfer enhancement of an automobile radiator using nanofluids. So I will explain the use of nanofluids in automotive in this research.

#### **1.4 Literature Review**

Stephen U.S. Choi et al, proposed that a new group of heat transfer fluids. These fluids are more thermal conductive as compared to conventional fluids. In many industrial applications less thermal conductivity is a basic problem in the development of heat exchange fluids. The nanofluids are engineered with suspension of metallic oxide nanoparticles in fluids. As the result these nanofluids are highly thermal conductive, so the nanofluids are new hope in heat exchange system that are used in many industrial applications and automobiles. They found the one of the benefit of nanofluid that is reduction of pumping power in heat exchange system. To double the heat transfer rate, the

pumping power required to increase 10 times for conventional fluid. But in case of nanofluids at the same pumping power the heat transfer rate was double [10].

Nanofluids-a basic word of the arising universe of nanotechnology-are suspensions of nanoparticles (significantly 1-100 nm in size) in regular base liquids like water, oils, or glycols. Nanofluids have seen tremendous development in prevalence since they were proposed by Choi in 1995. In the year 2011 alone, there were almost 700 exploration articles where the term nanofluid was utilized in the title, showing fast development from 2006 (175) and 2001 (10). The main ten years of nanofluid research was basically centered around estimating and displaying key thermophysical properties of nanofluids. Ongoing examination, be that as it may, investigates the presentation of nanofluids in a wide assortment of different applications [11].

The Heat exchange system is very important for automobile engine performance. Conventional coolant liquids, such as water, ethylene glycol, has poor heat transfer performance. For the enhancement of heat transfer, Nano fluids are the new window. Nano fluids are liquid suspensions containing metallic or nonmetallic oxide nanoparticles. Nanoparticles are significantly smaller than 100nm. Al<sub>2</sub>O<sub>3</sub> nanoparticles were added into the water and made five different concentrations in the range of 0.1 to 1vol%. These five different concentrations flows through the automobile radiator. The flow rate has been changing from 2 to 5 l/min. The fluid inlet temperature has been changing from 37 to 49 C, heat transfer coefficient had also analyzed. At 1vol% the Nano fluids in automobile radiator can enhance the heat transfer up to 45% as compared to pure water [12].

The performance of automobile radiators can be enhanced by using Nano fluids. Four different nanoparticles (Al<sub>2</sub>O<sub>3</sub>, TiO<sub>2</sub>, ZnO, and SiO<sub>2</sub>) mixed in water are used in an automobile radiator to check the heat transfer rate. CFD simulation is performed on Ansys fluent to check the effect of their properties on heat transfer rate. ZnO and Al<sub>2</sub>O<sub>3</sub> have better thermal properties as compared to TiO<sub>2</sub> and SiO<sub>2</sub>. For ZnO, the increase in heat transfer rate is maximum from

4.9% to 19%. The second option is Al<sub>2</sub>O<sub>3</sub> gives a heat transfer rate from 4% to 13%. TiO<sub>2</sub> and SiO<sub>2</sub> do not enhance the heat transfer rate [13].

In this study, the hydraulic and thermal properties of Nano fluids in radiator tubes were checked numerically. To calculate the thermal conductivity and viscosity of Nano fluid empirical correlation was used. Reynolds numbers were compared with different concentrations of nanoparticles in water and ethylene glycol at the same time Nussle numbers for those single and two-phase models were compared with experimental data. When the concentration of nanoparticles in water or ethylene glycol increases the heat transfer rate and Nussle number is increase. The effect of inlet temperature on Nussle number is shown that a two-phase model is better than a single phase for experimental data [14].

Due to the use of nanoparticles in base fluids (water or ethylene glycol) the process of resizing the automobile radiator is performed. In this process four (1, 3, 5, and 7%) different concentrations of Nano fluids were used at Reynolds number changes from 250 to 1750. In automotive radiator flat tubes (high surface to cross-sectional area ratio) has been recently introduced. Higher length (11.7%) reduction of the flat tube of car radiator achieves by using the Al<sub>2</sub>O<sub>3</sub>(7%) nanoparticles in the base fluid. While by using CuO nanoparticles in base fluid (water or ethylene glycol) 9.8% reduction of tube lengths is achieved. 75 to 80% of the pumping power is required when Nano fluid was used due to the friction of nanoparticles [15].

In this article, the heat transfer performance and the flow characteristic in a flat tube of a car radiator have been checked computationally with three distinct fluids: base fluid(water) and two water based Nano fluids (Al<sub>2</sub>O<sub>3</sub> and CuO nanoparticles in water) at different concentrations. This research addresses the drawbacks of high pumping power and benefits of enhanced heat transfer rate due to the use of Nano fluids. Nano fluids are not cost free Most previous studies used non-dimensional parameters that do not highlight about that. Addition of Al<sub>2</sub>O<sub>3</sub> and CuO nanoparticles in base fluid(water) can increase the heat transfer rate of the car radiator as compared to base fluid(water). The enhancement rate

of heat transfer coefficient is dependent on the amount of nanoparticles Al<sub>2</sub>O<sub>3</sub> and CuO added to base fluid(water). The enhancement in heat transfer coefficient reached 38 % and 45 % for CuO/water and Al<sub>2</sub>O<sub>3</sub>, respectively compared to the values of the base fluid(water). By increasing nanoparticles (Al<sub>2</sub>O<sub>3</sub> and CuO) concentration the pumping power and Pressure drop increase. By Adding nanoparticles (Al<sub>2</sub>O<sub>3</sub> and CuO) to a base fluid contributed to increase required pumping power in automobile radiator compared to the expected heat transfer coefficient enhancement. With more added particles to the fluid this preceding increases. Nano particles(Al<sub>2</sub>O<sub>3</sub>) in base fluid(water) achieves a higher length reduction than Nano particles(CuO) in base fluid, it is estimated that 9.8 % and 11.7 % reduction of tube length are achieved for CuO and Al<sub>2</sub>O<sub>3</sub> nanoparticles, respectively for same temperature difference and the cooling rate. where more 75 % and 80 % of the pumping power is needed for an automobile radiator so using of Nano fluids is not always beneficial. 7 % of Al<sub>2</sub>O<sub>3</sub> and CuO nanoparticles in base fluid(water) in an automobile radiator having flat tube with reduced length 9% and 12%, respectively removes same amount of heat as compared to base fluid(water) flowing in the radiator having original tube length. The ideal nanoparticle volume concentration which gives a reasonable heat transfer improvement with moderate pumping power rise is examined and approximately found to be 4.5 % for both Al<sub>2</sub>O<sub>3</sub> and CuO [16].

S.M. Peyghambarzadeh et al. compared the heat transfer performance of ethylene glycol and water and their different mixtures. Additionally, different concentrations of Al<sub>2</sub>O<sub>3</sub>(nanoparticles) was added into these base fluids water and ethylene glycol. Then the effects of Nano fluids on heat transfer performance of automobile radiator was determined experimentally. five different flow rates 2, 3, 4, 5, and 6 l/m was checked and the fluid inlet temperature was changed for all times when experiment was performed. With nanoparticles addition in base fluid the heat transfer rates had increased. Enhancement of nusselt number observed at best conditions up to 40% for both Nano fluids. He observed that heat transfer rate of Nano fluids is strongly dependent on Nano particle concentration in water and ethylene glycol and weakly dependent on inlet temperature [17].

K.B. Anoop et al. performed an experiment in which they studied the convective heat transfer. For that purpose, they applied the constant heat flux at the wall of tube. In this experiment the nanofluid was Alumina-water. The first objective of this research is to check the effect of nanoparticle size on convective heat transfer in the laminar regime. Two different sizes of nanoparticles were used 45nm and 150nm. In both cases the heat transfer rate increased as compared to base fluid like water and ethylene glycol. But the particle having size 45nm increase more heat transfer than the particle having size 150nm. It was also observed that when the particle concentration in base fluid increased the heat transfer coefficient increased. By using the nanoparticle in base fluid a correlation is was suggested in the developing region [18].

Mostafa et al. investigated that the convective heat transfer effect with constant heat flux on the Nano fluid flow in the developing region of a tube using CFD. For this purpose, four particle concentrations (1,2,4, and 6 wt %) of Nano particles Al<sub>2</sub>O<sub>3</sub> in water as a base fluid single phase with two average particle sizes (45 nm were used and 150 nm) were used. Five different axial location on the tube were selected. At different Reynold numbers( $500 < Re < 2500$ ) the convective heat transfer coefficient was investigated by changing the particle size. Data obtained from simulations in a very good agreement with experimental data that was obtained from literature. The results showed that with increasing the Nano particle concentration in base fluid and Reynold number the heat transfer coefficient was increased. Further, with increasing the Nano particle concentration in base fluid and particle diameter the heat transfer coefficient decreased [19].

S. Zeinali heris et al. studied that conventional coolant such as ethylene glycol and water are used in automobile radiators for heat transfer from engine to atmosphere, and these coolant fluid has relatively poor heat transfer rate. In their study, CuO nanoparticles were added into the mixture of ethylene glycol/water. And then the heat transfer performance of a radiator calculated. The thermal performance of a car radiator checked at different flow rates (4-8 liter/min), different concentrations (0.05-0.8vol%) of nanoparticles in base fluid and different inlet temperature. In the results of this study, the enhancement of NU



number achieved up to 55% when the concentration of nanoparticles is 0.8vol% in water-EG mixture. The NU number increases with the increase of volumetric concentration of Nanoparticles and flow rate. The heat transfer rate increase by using the nanofluid. Therefore, use of nanofluids provide a new way to engineers for development of effective radiators for automobiles [20].

Parashurama M S. et al. performed an experiment to check the thermal properties of single phase flow in army tank diesel engine radiator. For heat transfer in automobile engines radiator is important. In this study they attempt to study that, the thermal properties of CuO nanoparticles in water as a coolant. Heat transfer rate of automobile radiator checked at 10% concentration of copper oxide. In the results the heat transfer rate is maximum for copper oxide and heat transfer rate is lower for water. Furthermore, three different flow rates checked for optimum results of radiator. The results show that nanofluids have better thermophysical properties as compared to water [21].

Mohd Muzammil Zubair et al. studied the convective heat transfer coefficient of TIO<sub>2</sub>, EG and water Nano coolant. The base nanofluid made with 25% ethylene glycol, 75% water and low volume fraction of TIO<sub>2</sub> nanoparticles. When this experiment has performed the flow rate of coolant is changing from 30 to 180 LPH. The results get from nanofluids are better than the mixture of water and ethylene glycol. At 0.03% of TIO<sub>2</sub> nanoparticles concentration the heat transfer rate is maximum that is 29.5%. these results are obtained due to increase of heat transfer coefficient and thermal conductivity of nanofluid. For nanofluid the temperature difference is maximum of outlet and inlet of radiator than the mixture of water and ethylene glycol. We can clearly say that the thermal conductivity of nanofluids is better than the water and ethylene glycol. The temperature at outlet of the radiator is minimum when they used nanoparticles. This increase in heat transfer rate leads to the manufacturers of car radiator to develop smaller size and low cost radiator [22].

Dorin Lelea. Presented the numerical study of fluid flow of AL<sub>2</sub>O<sub>3</sub> nanoparticles in base fluid(water) and conjugate heat transfer rate. For this study laminar regime has considered. For the microchannel heat sink a square

microchannel has considered with hydraulic diameter that is 50 micro meter. In case of cooling and heating the heat flux was fixed  $35 W/m^2$ . The volume concentration of  $AL_2O_3$  nanoparticles is varying from 1 to 9%. For this numerical study three different particles diameter has selected that is  $d_p = 13, 28$  and  $47$  nm. For numerical prediction the homogenous model is used. Along the microchannel the heat transfer increased. When the particle diameter is increases the heat transfer rate increase. Moreover, for the low pumping power in case of heating the heat transfer rate is greater than the cooling case. The heat transfer rate is higher in case of nanofluid is cooled for high pumping power. In case of cooling along the microchannel the heat transfer rate decreased. When the particle diameter increases the heat transfer rate decreases [23].

Ravikanth, presented the new correlations. These correlations used for friction factor and convective heat transfer. The nanoparticles are mixture of silicon dioxide, aluminum oxide and copper oxide mixed in 40% water and 60% ethylene glycol mixture. The experimental results are obtained at fully developed turbulent regime. The thermophysical properties of nanofluids density, viscosity, thermal conductivity and specific heat were find by varying different volume concentration and temperature. For the development of heat transfer coefficient correlation from experiment these properties are used, as a function of volumetric concentration and these properties. The new correlation developed for friction factor of nanofluid and the pressure loss was also measure. When the volumetric concentration of nanofluids increase its increases the heat transfer coefficient. For example, when the Reynold number is 7240, for 10% volumetric concentration of aluminum oxide in base fluid the percentage increase in heat transfer coefficient is 81.74%. with an increase in volumetric concentrations of particle in base fluid the pressure drop increased. The pressure drop achieved 4.7 times greater than the base fluid when the particle concentration in the base fluid was 10% and the Reynold number was 6700. For single phase approach the new correlation developed for nusselt number similar to Gnielinski correlation. The new correlation is a function of prandtl number, volumetric correlation and Reynold number. For the friction factor the new equation developed [24].

Hossein Fatahian, studied the thermal effect of Nanoparticles in the water and fuel oil based fluid. These effects are studied in the channel by using fuel-oil-alumina and water-alumina nanofluids. For the solutions of equations, the second order method used. For pressure velocity coupling the simple algorithm was applied in fluent. At different Reynold number 900-2100, the effect of nanoparticle concentration and particle size on convective heat transfer coefficient was studied. The simulations performed for the different volume concentrations and nanoparticle size under constant heat flux in fully laminar regime. The results of these simulations showed that by increasing the volumetric concentration of nanofluid in base fluid results increase in the thermal conductivity of fluid. The increase in thermal conductivity ratio smaller degree in water alumina nanofluid than the fuel oil alumina nanofluid. The nusselt number increase by increasing the volume concentration of nanoparticles. It's also showed by increasing the volume fraction of nanoparticle the heat transfer coefficient of nanofluid also increased. In the same volume concentration, the effect of adding alumina nanoparticles in the water base flued has less effect than the adding alumina nanoparticles in fuel-oil base nanofluid. At the same volume concentration and Reynold number, when the particle size increase the heat transfer coefficient decreased [25].

K.V. Sharma et al. performed an experiment to calculate the friction factor and heat transfer coefficient in a tube. A twisted tape is inserted in the range where transition of flow occurs. The aluminum oxide nanoparticles are used. The results shows the enhancement of convective heat transfer for  $AL_2O_3$  nanoparticles as compared to water. It is observed that for single phase approach the correlation of gleninski is good for transnational range of flow. For single phase approach show some deviation of values when compare these values with nanofluid. At 9000 re number the nanofluid passing through the tube with 0.1% volume concentration the convective heat transfer coefficient is 23.7% higher as compare to water. At 300 Reynold number the heat transfer coefficient enhancement of aluminum oxide nanoparticles is 13.77% at 0.1% volume concentration [26].

Many researchers work on the enhancement of thermal conductivity of coolant. However, to investigate the heat transfer coefficient of coolant a huge amount of publications is available. Weerapun Duangthongsuk et al, study the heat transfer behavior of nanofluids.  $TiO_2$  nanoparticles dissolved in water was in under consideration [27]. Yimin Xuan et al, investigated that the nanofluids enhance the thermal conductivity and heat transfer of coolant. Nanofluids are a new type of medium, in heat transfer coolants [28]. M. Naraki et al, performed an experimental study on heat transfer coefficient of an automobile radiator. They found that the heat transfer decreased with increasing the outlet temperature of engine coolant. Using of nanofluids instead of base coolant(water) increase the thermal performance of an automobile radiator [29]. B. Farajollahi et al, investigated the heat transfer behavior of  $TiO_2$  and  $AL_2O_3$  in a tube heat exchanger. They found that  $AL_2O_3$  have better heat transfer properties at higher volume concentrations. At different volume concentrations both nanofluids heat transfer enhancement had not same.

## 1.5 Research Gap

After comprehensive literature review on application of nanofluids as performance enhancement agents. Following research gap is identified.

- i. Limited numerical studies are available on the effects of coolants
- ii. CFD studies on the subject are limited to 2D and 3D tubes
- iii. Effects of adding Nanoparticles on mass flow rate is not addressed

## 1.6 Objectives

To address the gap identified in previous section. Current study has following research objectives to fill gaps in some of the identified areas:

- i. To simulate the working principle of liquid-based radiator
- ii. To correctly simulate the flow physics of adding Nanoparticles in the radiator coolant
- iii. Effect of different nanoparticles on the performance of the radiator
- iv. Effect of nanoparticles volume concentration on the performance of the radiator

Computational Setup

2.1 Geometry

Rectangular tubes down flow radiator is used for this study. Ngoctan Tran et al [30], studied the effect of different tubes shape at the performance of different heat exchange systems. In their study they conclude that, the thermal performance of rectangular tube is greater than the square shaped tube. For the simplicity of geometry and meshing, we select rectangular tubes in the radiator. The main core of the radiator consists of 34 vertical aluminum tubes.

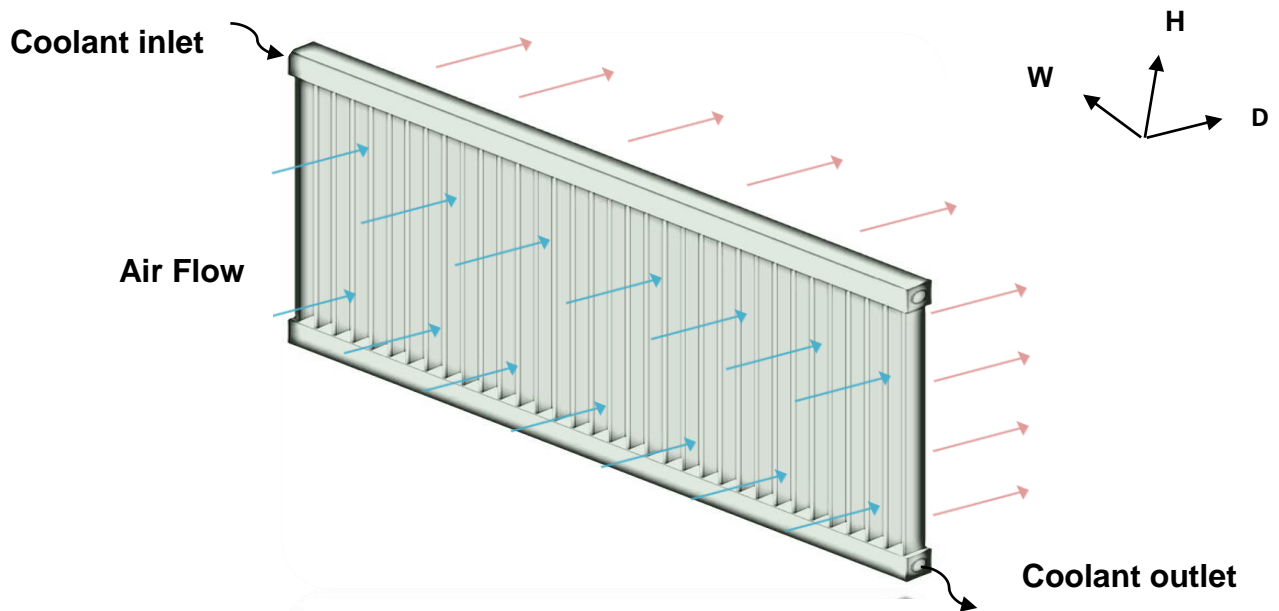


Figure 2.1 Radiator geometry

Aluminum metal is used in manufacturing of the radiator, it's a down flow radiator [21]. In an automobile air from the atmosphere hit the surface of radiator. Cooled air from the atmosphere produce natural convection at the wall of radiator tubes. And extract the heat from radiator tube surface. Cooled air change into hot air due to convection at the wall of radiator tubes. Due to convection at wall of tubes the heat is extracted from coolant, that is running in the radiator and engine and then the cooled liquid return back to the engine.

The dimensions of the radiator are as follows:

- i. Depth=24mm.
- ii. Width=605mm.
- iii. Height=370mm.

Whereas the dimensions of the radiator tubes are:

- i. Depth=20mm.
- ii. Width=3mm.
- iii. Height=310mm.

These dimensions of the tubes are obtained from [21]. In [21], they performed an experiment on car radiator to check the heat transfer rate of  $Al_2O_3$  nanofluids.

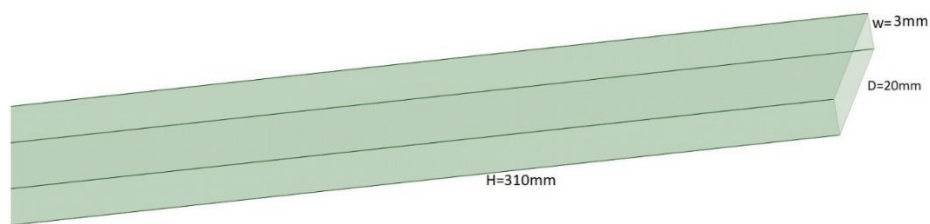


Figure 2.2 3D Rectangular tube of radiator

## 2.2 Computational Fluid Dynamics

Computational fluid dynamics (CFD) is a process, in which we investigate the fluid flow problem by using numerical analysis in computer. Boundary conditions defines the interaction of surfaces and walls with fluid flow. High speed computers are required in most complex problems of computational fluid dynamics. CFD is applied at different analysis of engineering problems and many fields of applied sciences, including aerodynamics, heat transfer analysis, and combustion analysis.

### 2.2.1 Introduction to ANSYS Fluent

Ansys Fluent used a three-dimensional finite volume method to numerically solve the incompressible time-dependent Navier-Stokes equations.

### 2.2.2 Pressure Based Solver

In Fluent we have two options i.e. density based solver and pressure based solver for numerical method. Pressure based solver is preferred for incompressible regime low Mach number  $< 0.3$  , while density based solver is generally used for high Mach number [31] correspond to compressible regime.

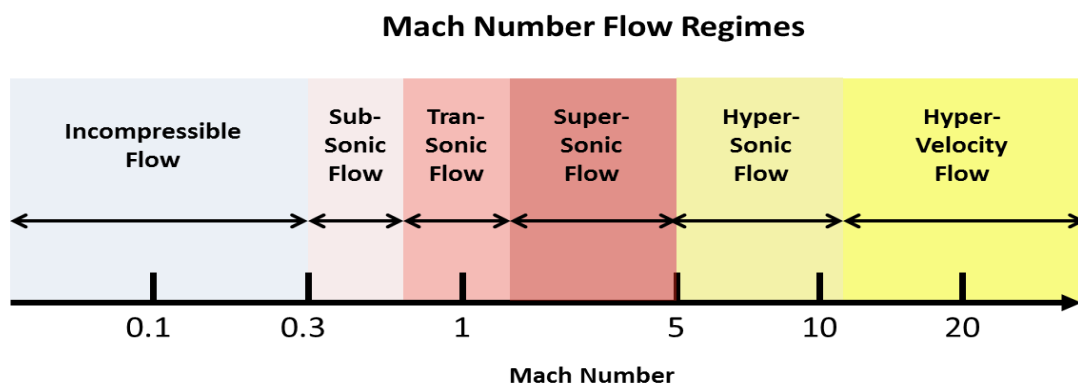


Figure 2.3 Mach number with flow regime

Flow rate	Density of water	Viscosity of water	Inlet diameter	Inlet area	Inlet velocity	Inlet Reynold number
4	998.2	0.001003	0.015	0.000176	0.379006	5657.89
5					0.473758	7072.362
6					0.56851	8486.834
7					0.663216	9091.307
8					0.758013	11315.78

Table2.1 Calculation for base fluid

For the present study pressure based solver is selected because the Mach number is less than 0.3. The main domain of the radiator model split into discrete control volumes. Through discretization algebraic equations are obtained in terms of unknown variables. To achieve the convergence of these algebraic equations iterative method is required. Energy equation is turned on from Fluent graphical user interface because present study focused the heat transfer in automobile radiator.

For a control volume, consider the so-called transport equation [34] that is given below.

$$\int_v \frac{\partial \rho \phi}{\partial t} dV + \oint \rho \phi \vec{v} \cdot d\vec{A} = \oint \rho \phi \vec{v} \cdot d\vec{A} + \int_v s_\phi dV \quad 2.1$$

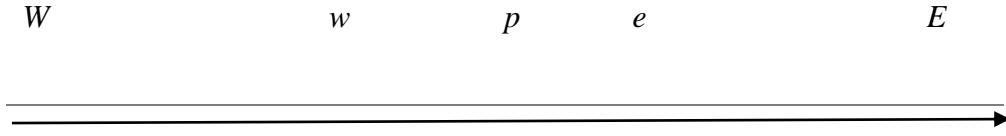
In equation 2.1 the first term on the left hand side represent the rate of increase in  $\phi$  in a closed volume. The second term on the left hand side represent the convection across the boundaries of control volume as a result it represent the rate of decrease of  $\phi$ . The third term on the right hand side of the equation represents the rate of increase in  $\phi$  because the diffusion across the boundaries of control volume. The fourth equation on the right hand side of equation 2.3 represent the rate of forming of  $\phi$  as a result of source inside the control volume. In computational domain equation 2.1 is applied at each control volume.

### 2.2.3 Discretization

Fluent save the value of  $\phi$ ( scalar quantity) at the center of a cell but the value of  $\phi$  is required at the face of the cell for convective terms that are in the governing equation. Due to requirement of value at faces of cells it is calculated by different schemes. At high peclet numbers central difference scheme does not own the Transportiveness property of discretization scheme. While first order upwind difference scheme increases the convergence of numerical



solution but it not tells about the flow direction. In the present study I prefer the second order upwind scheme for discretization.



Consider the fluid is flowing from west to east, and we want the value of  $\phi$  at face e. Second order upwind scheme contains two points from upstream.

$$\phi_e = \phi_p + \left( \phi_p + \frac{\phi_p}{\delta x} \right) \cdot \delta x / 2 \quad 2.2$$

### 2.2.4 Pressure Velocity Coupling

Navier-Stokes equations are non-linear partial differential equations that are used in Fluent to solve the CFD problem. Consider a case in which the flow is laminar and no source term is included.

The  $x - momentum$  equation:

$$\begin{aligned} \frac{\partial \rho v_x}{\partial t} + \frac{\partial \rho v_x^2}{\partial x} + \frac{\partial \rho v_x v_y}{\partial y} + \frac{\partial \rho v_x v_z}{\partial z} & \quad 2.3 \\ = \frac{1}{R_e} \left[ \frac{\partial \tau_{xx}}{\partial x} + \frac{\partial \tau_{xy}}{\partial y} + \frac{\partial \tau_{xz}}{\partial z} \right] - \frac{\partial p}{\partial x} \end{aligned}$$

$y - momentum$  equation:

$$\begin{aligned} \frac{\partial \rho v_y}{\partial t} + \frac{\partial \rho v_x v_y}{\partial x} + \frac{\partial \rho v_y^2}{\partial y} + \frac{\partial \rho v_y v_z}{\partial z} & \quad 2.4 \\ = \frac{1}{R_e} \left[ \frac{\partial \tau_{yx}}{\partial x} + \frac{\partial \tau_{yy}}{\partial y} + \frac{\partial \tau_{yz}}{\partial z} \right] - \frac{\partial p}{\partial y} \end{aligned}$$

And  $z - momentum$  equation:

$$\begin{aligned} \frac{\partial \rho v_z}{\partial t} + \frac{\partial \rho v_z v_x}{\partial x} + \frac{\partial \rho v_z v_y}{\partial y} + \frac{\partial \rho v_z^2}{\partial z} & \quad 2.5 \\ & = \frac{1}{Re} \left[ \frac{\partial \tau_{zx}}{\partial x} + \frac{\partial \tau_{zy}}{\partial y} + \frac{\partial \tau_{zz}}{\partial z} \right] - \frac{\partial p}{\partial z} \end{aligned}$$

Continuity equation

$$\frac{\partial \rho}{\partial t} + \frac{\partial \rho u}{\partial x} + \frac{\partial \rho v}{\partial y} + \frac{\partial \rho w}{\partial z} = 0 \quad 2.6$$

In equations 2.3-2.6  $v_x$   $v_y$   $v_z$  represent the velocity and  $p$  represent the pressure and  $x$ ,  $y$  and  $z$  represent the direction components. The continuity and momentum equations are linked each other because the velocity component appears in both equations. For compressible flows, to obtain the value of pressure field we use the ideal gas law  $p = \rho * R * T$ . However, in case of incompressible flows this case is not valid because the pressure is not linked with density. Simplec, Simple and PISO iterative algorithm are used to resolve the pressure velocity coupling.

Generalized energy equation

$$\begin{aligned} \frac{\partial E_T}{\partial t} + \frac{\partial v_x E_T}{\partial x} + \frac{\partial v_y E_T}{\partial y} + \frac{\partial v_z E_T}{\partial z} & \quad 2.7 \\ & = - \frac{\partial v_x p}{\partial x} - \frac{\partial v_y p}{\partial y} - \frac{\partial v_z p}{\partial z} \\ & - \frac{1}{Re Pr} \left[ \frac{\partial q_x}{\partial x} + \frac{\partial q_y}{\partial y} + \frac{\partial q_z}{\partial z} \right] \\ & + \frac{1}{Re} \left[ \frac{\partial}{\partial x} (v_x \tau_{xx} + v_y \tau_{xy} + v_z \tau_{xz}) + \frac{\partial}{\partial y} (v_x \tau_{yx} \right. \\ & \left. + v_y \tau_{yy} + v_z \tau_{yz}) + \frac{\partial}{\partial z} (v_x \tau_{zx} + v_y \tau_{zy} + v_z \tau_{zz}) \right] \end{aligned}$$

## 2.2.5 Boundary Conditions

At the boundary of physical model, we apply the boundary conditions to define the flow parameter. The outlet temperature of the radiator is observed at outlet surface of the radiator. The outlet temperature is observed at different flow rates

4,5,6,7,8 L/min. simulations are carried out at different inlet temperatures of fluid 50,54,60 C. inlet of the radiator is fixed at velocity inlet from fluent graphical user interface GUI. Forced convection boundary conditions is applied at the wall of radiator tubes that are exists in the main core of radiator. The value of heat transfer coefficient is changing with the change of mass flow at inlet. In [14] vahid et al, applied the convection boundary conditions at the wall of tubes, the value of heat transfer coefficient is  $150 \text{ W}/\text{m}^2\text{K}$  and ambient temperature is 303k. At the surface of main core(tubes), no slip conditions apply its means that no relative motion between the fluid layer and wall.

### **2.2.6 Turbulence Model**

Turbulence is produced due to the irregular pattern of flow in which swirls and eddies are generated. For the CFD analysis of turbulence flows, the Navier-Stokes equations can be time average. The Reynold average Navier-Stokes equations is used to remove the small fluctuations. The new equations contain the more unknowns and to solve the system of equations we required the turbulence model.

In this study, the radiator is run at different flow rates 4,5,6,7 and 8 L/min with K- $\epsilon$  turbulence model and Spalart-Allmaras model. Spalart-Allmaras model is one equation model so it is computationally less expensive. K- $\epsilon$  turbulence model and Spalart-Allmaras model are eddy viscosity models. In RANS less mesh density is required to solve these models so they are less computationally intensive. These models, model all the turbulence, in the results they are less accurate.

### 2.2.7 Calculation of $Y^+$

$Y^+$  is used to correctly simulate the flow physics near the wall of model. Mathematical formula of  $Y^+$  is:

$$Y^+ = \frac{\rho * u * y}{\mu} \quad 2.8$$

Where

$$u = \text{friction velocity of fluid} = \sqrt{(Tw / \rho)}$$

$y$  = distance of first cell from the wall

for the calculation with Spalart-Allmaras model, it is endorsing that the value of  $Y^+$  is equal to 1. Because the main reason behind this is that Spalart-Allmaras model is designed for meshes that is used to solve the viscous affected regions.

### 2.2.8 Computational Resources

As we know that, the model is used for simulation is 3D radiator. High computational setup is required for this heavy mesh. The processor is used for 3 dimensional modeling and meshing is Intel(R) Core(TM) i7-9700 CPU @ 3.00GHz 3.00 GHz with 16gb RAM.

## 2.3 Theory and Related Works

In this section, we will discuss the basic formulas that are used to find the Nusselt number Reynold number, heat flux, heat transfer coefficient and mass flow rate.

$$\dot{m} = \rho * v * A \quad 2.9$$

In equation 2.9 [32] where

$v$ =velocity of water

$A$ = inlet area of radiator.

Equation 2.1 is used to calculate the inlet velocity of fluid when mass flow rate is given.

$$Re = \rho * u * D_h / \mu \quad 2.10$$

In equation 2.10 [33] where

$u$  = velocity of fluid

$D_h$  = hydraulic diameter of radiator.

$\mu$  = viscosity of water.

Equation 2.10 [34] is used to find the Reynold number at inlet of radiator.

$$Nu = \frac{hL}{k} \quad 2.11$$

In equation 2.11 [35] where

$L$  = characteristic length

To find the nusselt number equation 2.11 is used.

$$h = \frac{q}{\Delta T} \quad 2.12$$

$q$  = heat flux,  $\frac{w}{m^2}$

$\Delta T$  = Temperature difference between solid surface and suurounding of solid surface

Equation 2.12 [36] is used to find the heat transfer coefficient. Equation 2.13 [36] is used to find the heat flux. Equation 2.14 represent the relationship between mass flow and heat transfer.

$$q = -k \frac{dT}{dx} \quad 2.13$$

$$\Delta Q = m^{\circ} C_p \Delta T \quad 2.14$$

## 2.4 Validation with 2D Case

A 2D tube is selected from the literature for validation. In [19] mostafa used a 2D tube for his research.



Figure 2.4 Schematic of 2D tube

### 2.4.1 Grid Independence

A 2D grid is generated for the validation. The grid is generated using ICEM-CFD. In Fig. 2.5 10 cells along the radial direction is selected. And 1200 cells along the axial location is selected. Along the radial direction the spacing ratio is 1.1 to correctly capture the boundary layer along the wall. Along axial direction 1.1 spacing ratio is applied at inlet.

Cells	Faces	Nodes	Partitions
10791	22790	12000	4

Table 2.3 Size information of Mesh I

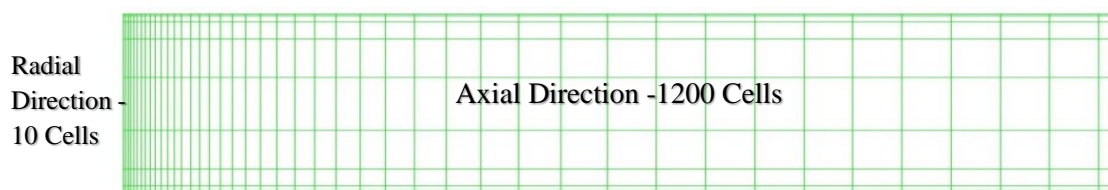


Figure 2.5 Mesh I

2nd mesh is generated by using the tools of ICEM-CFD. In Fig. 2.6 25 cells along the radial direction is selected. And 2000 cells along the axial location is selected. Along the radial direction the spacing ratio is 1.1 to correctly capture the boundary layer along the wall. Along axial direction 1.1 spacing ratio is applied at inlet.

Cells	Faces	Nodes	Partitions
47976	97975	50000	4

Table 2.4 Size information of Mesh II

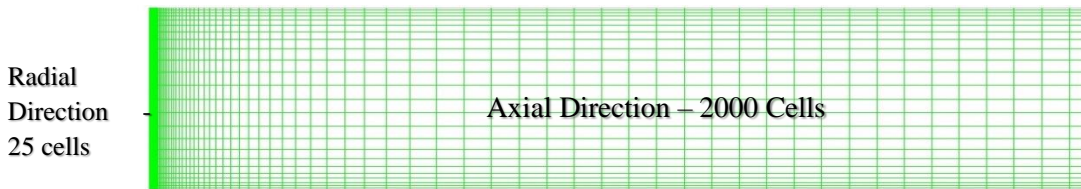


Figure 2.6 Mesh II

Cells	Faces	Nodes	Partitions
195951	395950	200000	4

Table 2.5 Size information of Mesh III

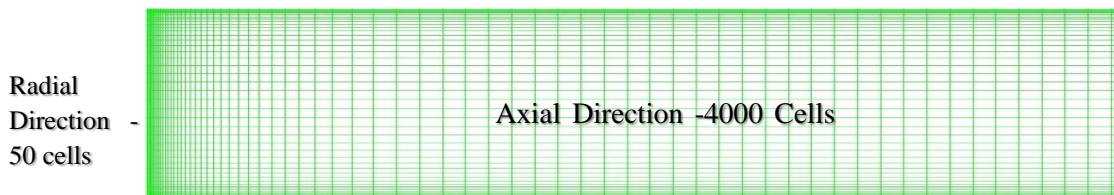


Figure 2.7 Mesh III

Fig. 2.7 represent the mesh3, this mesh is generated in ICEM-CFD. 50 cells along the radial direction is selected, and 4000 cells along the axial locations are selected. This mesh consists of 200000 nodes. At inlet edge 1.1 ratio is applied and at the wall edges 1.1 spacing ratio was also applied. Three grids with different combinations is selected for grid independence. The reason of grid independence is that to achieve the point where we increase the mesh size but the solution does not change.

#### 2.4.2 Boundary Conditions

To numerically solve the PDE'S we need the boundary conditions. Boundary conditions are applied in ANSYS Fluent. In Fig. 2.8 the domain of model is split up into 4 parts inlet, outlet, walls and fluid. Constant heat flux is applied at the walls. The inlet temperature of fluid is 286.5. No slip boundary conditions are applied at the walls. The inlet boundary condition is considered to be

velocity inlet and outlet is pressure outlet. The steady and incompressible flow conditions are considered for simulations. The flow is in laminar condition because the Reynold number is very low  $Re < 1600$

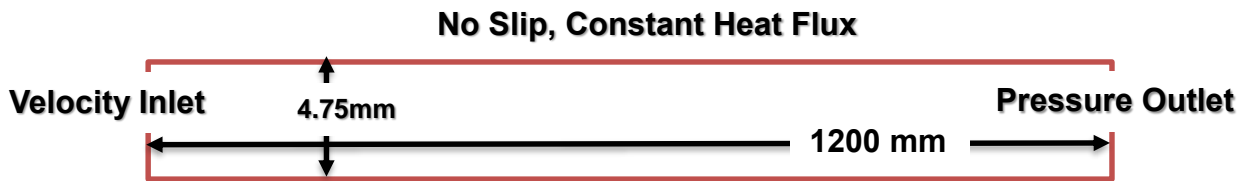


Figure 2.8 Boundary conditions

### 2.4.3 Simulations Results

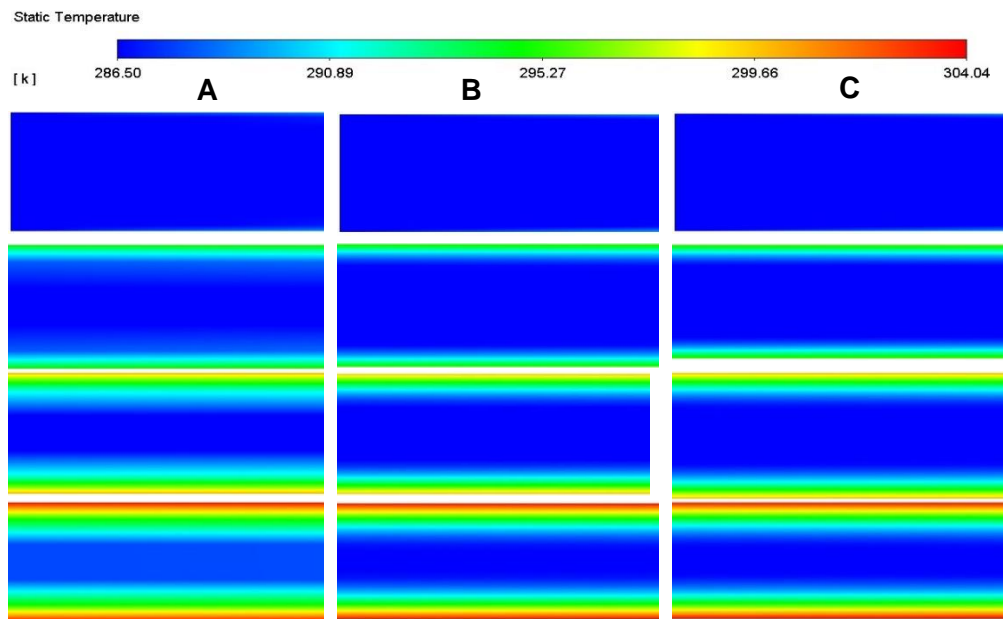


Figure 2.9 Contours of static temperature

Fig. 2.9 represents the contour of static temperature obtained by three simulations at different meshes. Side A of Fig. 2.9 represents the contours of static temperature simulated by using mesh1. Side B and C shows the contours of static temperature by using mesh 2 and 3 respectively.

Fig. 2.10 shows the sum of square of error of three results of simulations with mostafa[19] simulations. From the graph we can clearly see that the SSE of mesh2 is less than mesh1. Mesh3 contains 200000 nodes and the value of error



is nearly equal to mesh2, but due to large size of nodes the mesh3 consume more computational time as compare to mesh2. Hence mesh2 is better for further simulations.

Five different axial locations were selected at 2D tube to find the heat transfer coefficient  $h$ . The locations are 63, 105, 147, 200 and 244  $x/d$ . Fig. 2.10 shows the heat transfer coefficient with axial locations. In the graph we can clearly see that along the axial location the heat transfer coefficient is in decreasing order. In graph2 the simulations result by using water in a good agreement with mostafa [19] results.

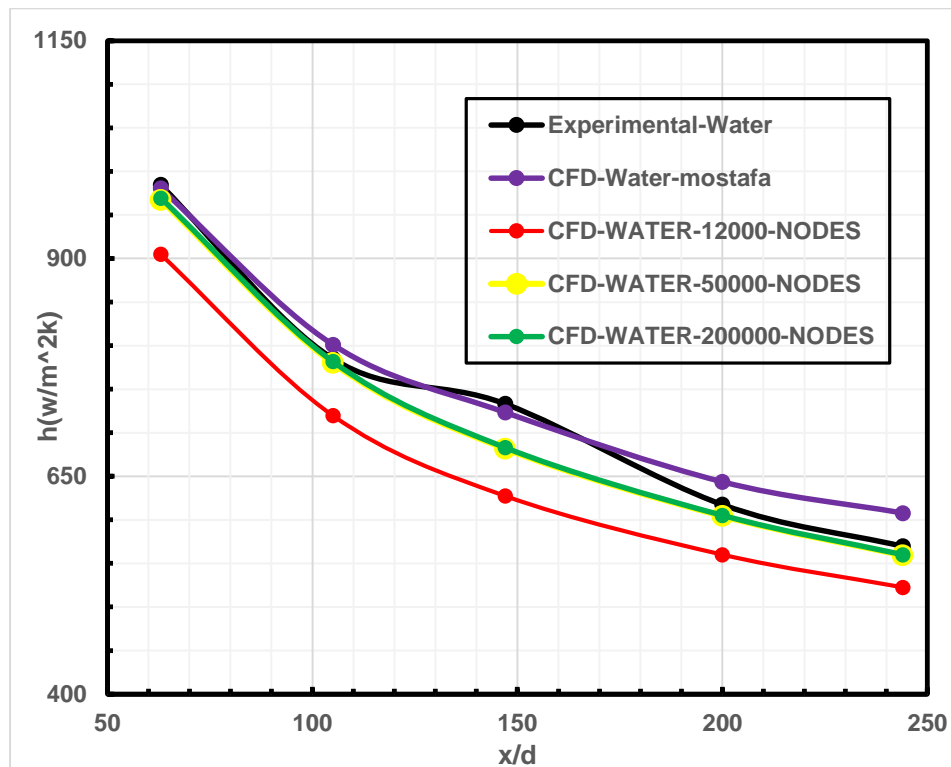


Figure 2.10 Heat transfer coefficient at different axial locations.

Fig. 2.10 represents the heat transfer coefficient with axial locations for nanofluids. In Fig. 2.11 results are similar as pervious graphs represent that, the heat transfer coefficient decrease along the axial location of 2D tube. Equation 2.11-2.14 are used to find the thermophysical properties of nanofluids. 4% volumetric concentration of  $AL_2O_3$  nanoparticles are used in base fluid water.

$$\rho_{nf} = \varphi \cdot \rho_p + (1 - \varphi) \cdot \rho_w \quad 2.11$$

$$(\rho C_p)_{nf} = \varphi \cdot (\rho C_p)_p + (1 - \varphi) \cdot (\rho C_p)_w \quad 2.12$$

$$\mu_{nf} = \mu_w(123\varphi^2 + 7.3\varphi + 1) \quad 2.13$$

$$K_{nf} = \frac{K_p + (n - 1)K_w - \varphi(n - 1)(K_w - K_p)}{K_p + (n - 1)K_w + \varphi(K_w - K_p)} K_w \quad 2.14$$

In equation 2.11, 2.12, 2.13 and 2.14

$\rho_{nf}$  = density of nanofluids.

$\varphi$  = volumetric concentration of nanoparticles in base fluid.

$\rho_w$  = density of water/base fluid.

$C_p$  = specific heat capacity of nanoparticle.

$\mu_{nf}$  = viscosity of nanofluid.

$\mu_w$  = viscosity of water/base fluid.

$K_{nf}$  = thermal conductivity of nanofluid.

$K_p$  = thermal conductivity of nanoparticles.

$K_w$  = thermal conductivity of water/base fluid.

$n$  = empirical shape factor which is consider to be 3.

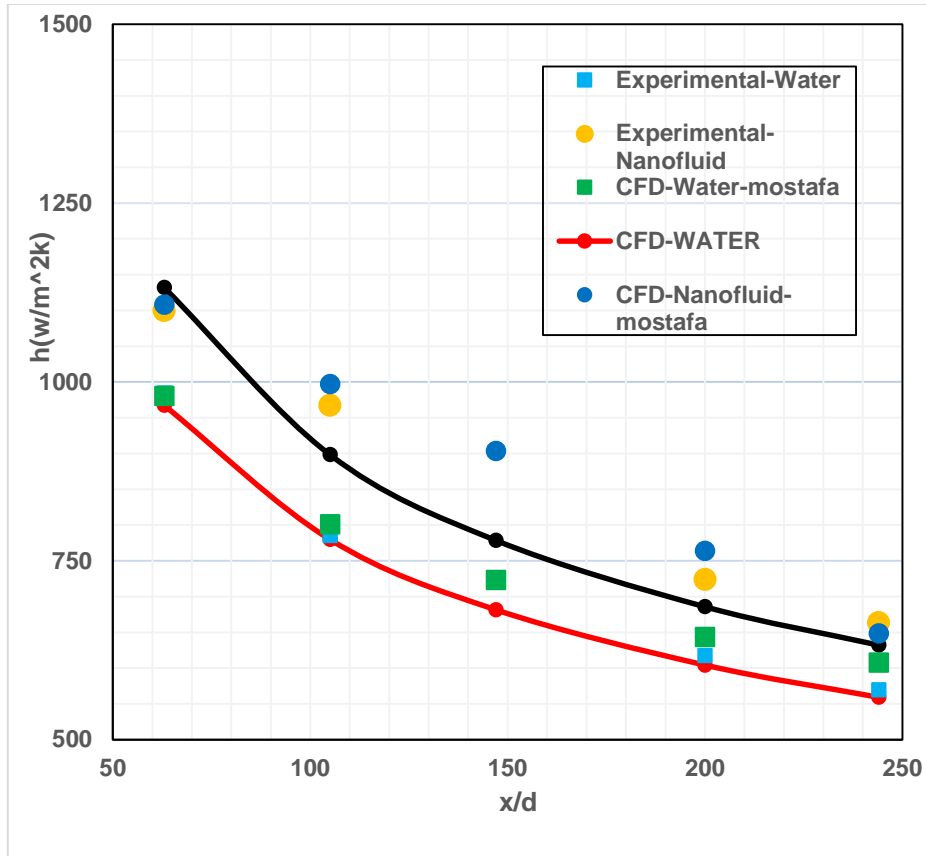


Figure 2.11 Heat transfer coefficient at axial locations of 2D tube.

## 2.5 Validation with 3D Case

### 2.5.1 Mesh of Radiator

The mesh of radiator is generated by using the tools of ICEM-CFD. Mesh of radiator consist of 0.8 million structured cells. Mesh is split up into four partitions inlet, outlet, walls and fluid. For structured meshing in ICEM-CFD the 3D bounding box is created for blocking. And then the 3D bounding box was split into small boxes for upper, lower and tubes. After the split each edge of radiator model is associated to block edge by associate vertex, associate edge to curve etc. After applying the spacing ratio near the tubes at cylinder 0.8million structured cells was generated.

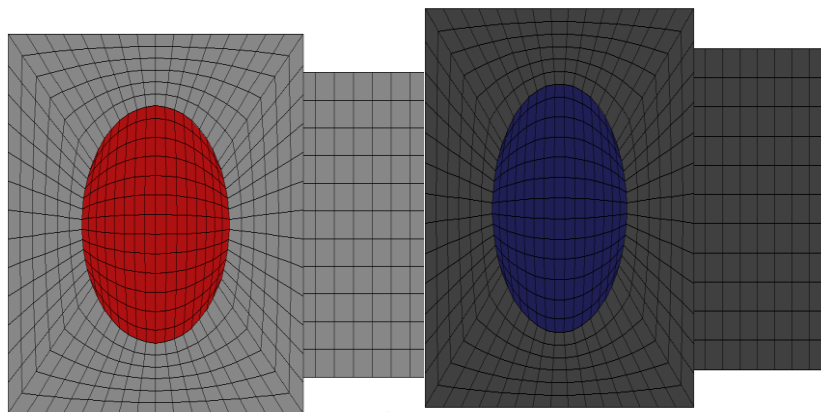
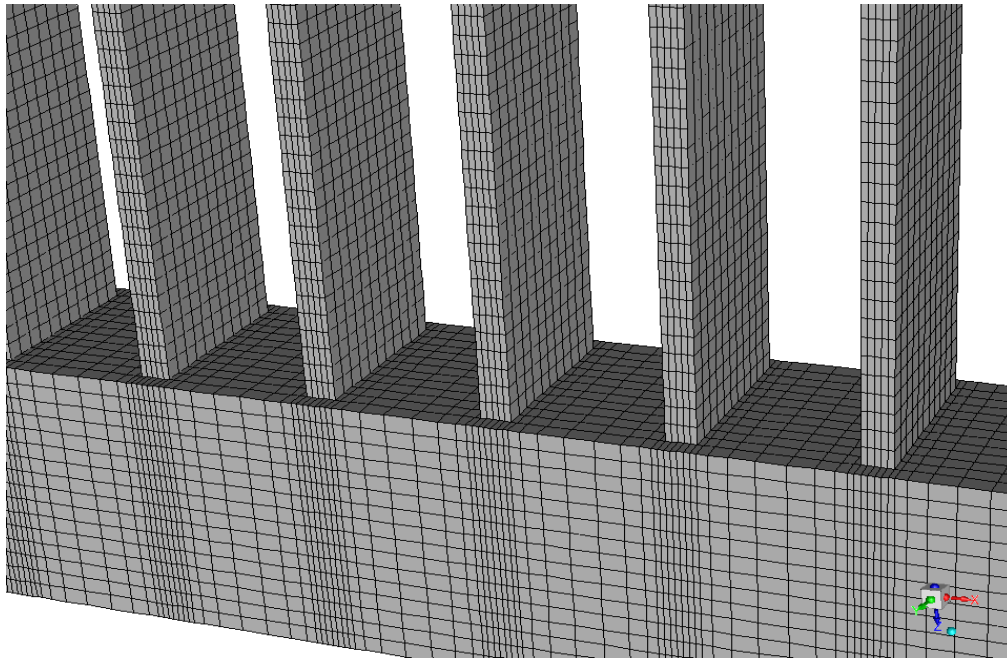


Figure 2.12 Structured grid of Radiator

Fig. 2.12 represents the structured grid at cylinder, tubes, inlet and outlet.

Cells	Faces	Nodes	Partitions
812697	2549045	929364	4

Table 2.6 Size information of radiator mesh.

### 2.5.2 Boundary Conditions

Boundary conditions are applied in FLUENT. The inlet temperature of coolant used in radiator is 327k [12]. Four different Reynold number is used for validation. The Reynolds number are 9500, 14267, 19034 and 23780. Forced convective boundary conditions are applied at the walls of radiator main core. The forced convective boundary condition is  $150 \frac{w}{m^2k}$  and ambient temperature

is 303k [14]. From the literature [12,29] we can say that by increasing the volume metric flow rate the heat transfer coefficient is increase. So by increasing the Reynold number 9500, 14267, 19034 and 23780 I increased the heat transfer coefficient value from  $150\frac{W}{m^2k}$  ,  $185\frac{W}{m^2k}$  ,  $225\frac{W}{m^2k}$  to  $265\frac{W}{m^2k}$  respectively while the ambient temperature is 313k same for all calculations.

### 2.5.3 Simulations Results

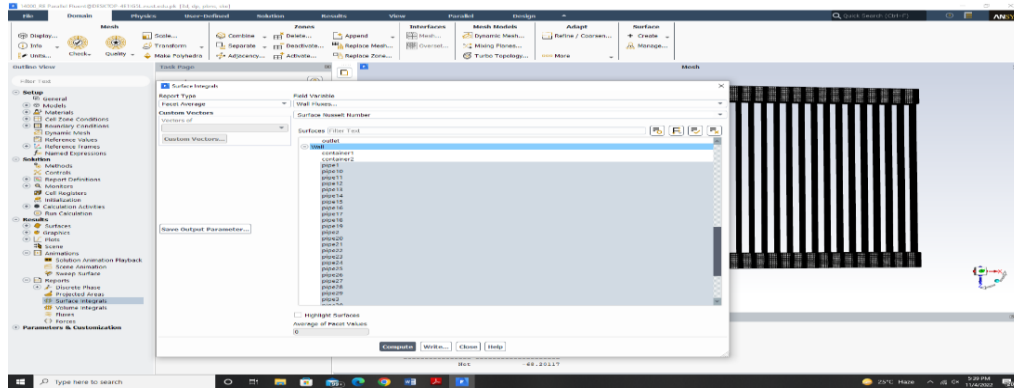


Figure 2.13 Nusselt number calculation in fluent.

Fig. 2.13 shows, how to calculate the surface nusselt number in FLUENT. In Fig. 2.14 when we increase the Reynold number the nusselt number is increase. For 3D validation purpose the Fig. 2.14 is in good agreement with peyghambarzadeh experiment [12]. The results of simulations show the average error with peyghambarzadeh is 0.97%.

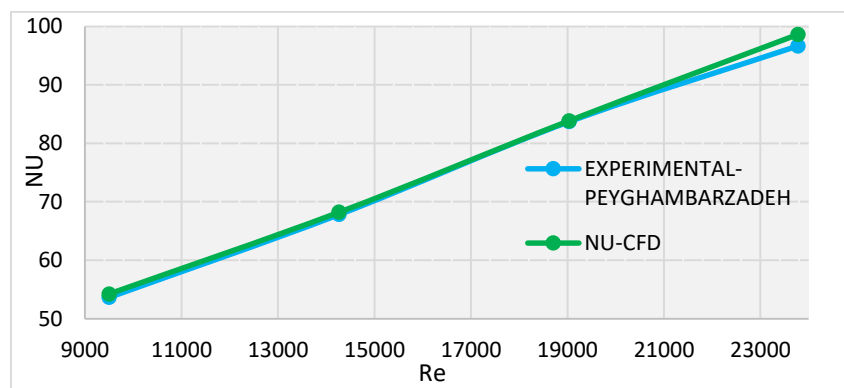


Figure 2.14 Nusselt number comparison of CFD simulation with experimental results for pure water.

### Simulations Results at Different Coolant Temperatures

#### 3.1 Introduction

In chapter 3 we simulate the radiator model at different temperature of coolant. For the simulations of different temperatures, I used the water as a coolant. Because in daily routine we use water as a coolant in automobile radiators. We will perform the simulations at forced convective boundary conditions. In this chapter we check the effect of inlet temperature at outlet temperature of radiator. When we obtained the results, we will insert a bar chart to check at which inlet temperature the radiator performs better at forced convective heat transfer conditions.

#### 3.2 Boundary Conditions

In chapter 2 we discussed about the mesh and model of radiator. So now we are discussing the boundary conditions. The boundary conditions are applied in Ansys Fluent. Four different inlet temperatures of coolant applied at inlet of the radiator, that's are 45, 50, 55 and 60 C. The five simulations performed for each inlet temperature. These five simulations are different flow rates of coolant 4, 5, 6, 7 and 8  $l/min$ . Fixed convection boundary conditions are applied at the walls of radiator. The value of convective heat transfer coefficient is  $150 W/m^2k$  and the ambient temperature is 303k for all cases.

### 3.3 Results

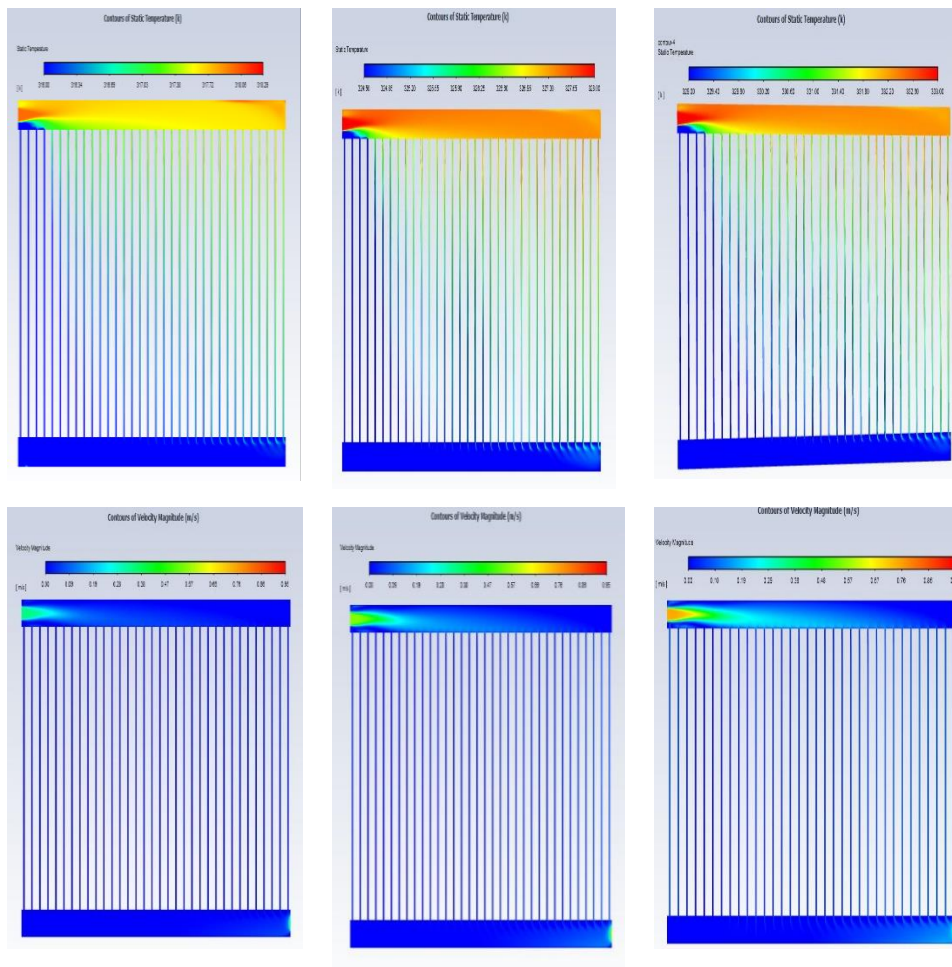


Figure 3.1 Contour plots of static temperature and velocity magnitude.

Fig 3.1 demonstrate the contour plots of velocity magnitude and static temperature. The first figure of row1 represent the temperature distribution at different inlet temperatures 45, 55 and 60 respectively. In the second row we can the contor plots of velocity magnitude at different flow rates, that's are 4, 6 and 8 l/min.

Fig 3.2 (a) and (b) demonstrates the outlet temperature with respect to flow rate at different inlet temperatures. When the flow rate increases the outlet temperature of radiator coolant is increase. Fig 3.2 (c) and (d) represents the outlet temperature of radiator with respect to inlet temperature at fixed flow rate. Fig 3.2 (c) the flow rate of inlet fluid is  $5 \text{ l}/\text{min}$  and in 4.2 (d) the flow rate of

inlet coolant is  $6 \text{ l}/\text{min}$ . From the graph it's clear that the outlet temperature of radiator increases by increasing the inlet temperature of coolant.

Fig 3.3 shows the temperature reduction of water at different inlet flows. The temperature reduction is inversely proportional to flow rate and directly related to inlet temperature of coolant.

Fig 3.4 represents the heat transfer coefficient with flow rate at different inlet temperatures. The heat transfer coefficient of radiator increases by increasing the flow rate of inlet coolant. The heat transfer coefficient  $h$  increases with the increase of inlet temperature of coolant. These results are obtained under fixed convective boundary conditions.

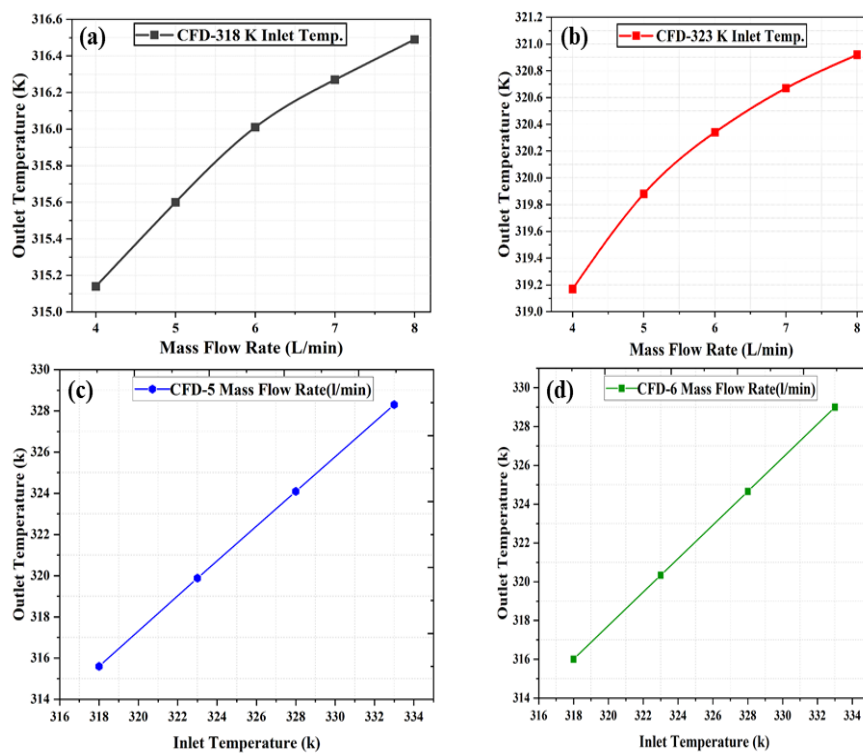


Figure 3.2 (a) and (b) represent the outlet temperature w.r.t. Mass flow rate. (c) and (d) represents the outlet temperature w.r.t. Inlet temperature.



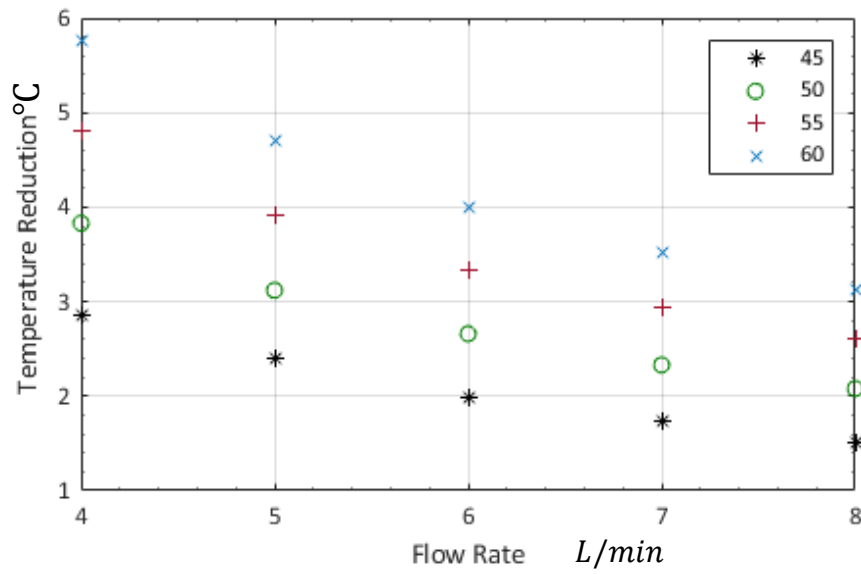


Figure 3.3 the temperature reduction of water at different inlet temperatures.

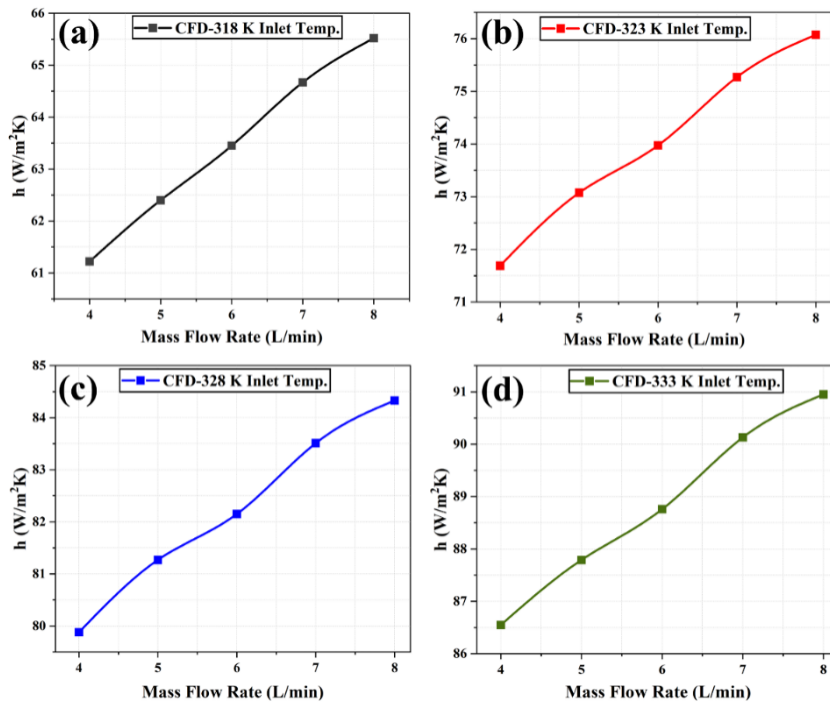


Figure 3.4 Heat transfer coefficient with flow rate of coolant.

### 3.4 Concluding Remarks

The following are the concluding remarks of chapter 3.

- i. The outlet temperature of radiator checked at different 45C, 50C, 55C and 60C inlet temperature.
- ii. Forced convection boundary conditions  $h=150 \text{ W}/\text{m}^2\text{k}$  are applied at the walls of radiator.
- iii. The outlet temperature of the radiator increases by increasing the flow rate.
- iv. When we increase the inlet temperature of coolant, the difference between the first and last value of outlet temperature increased, obtained at different flow rates.
- v. The maximum difference between the first and last value of outlet temperature achieved at 60C inlet temperature.
- vi. We achieved the maximum temperature reduction of water is 5.8°C when the inlet temperature of coolant is 60°C.
- vii. The temperature reduction is inversely related to the mass flow rate.
- viii. The temperature reduction is directly related to inlet temperature of coolant.
- ix. When we increase the flow rate the heat transfer coefficient is increase, this is the same result given in [12].
- x. The heat transfer coefficient increases by increasing the flow rate.
- xi. Heat transfer coefficient also increases by increasing the inlet temperature of coolant.

## Simulations Results for Different Nanofluids

### 4.1 Introduction

In this chapter we simulate the whole radiator by using different coolant. For this purpose, we simulate the pure water and different concentrations of nanoparticles in base fluid. The two types of nanoparticles are used in the simulations. The nanoparticles are  $Al_2O_3$  and  $CuO$ . These simulations are calculated at different flow rates. In this chapter we will discuss the change in outlet temperature of radiator by changing the value of flow rate and nanoparticles concentration in water.

### 4.2 Boundary Conditions

The mesh and model are same as discuss in previous chapter in section 3D validation. While the boundary conditions are different. The inlet temperature of coolant is 54 C.

### 4.3 Contours Plots

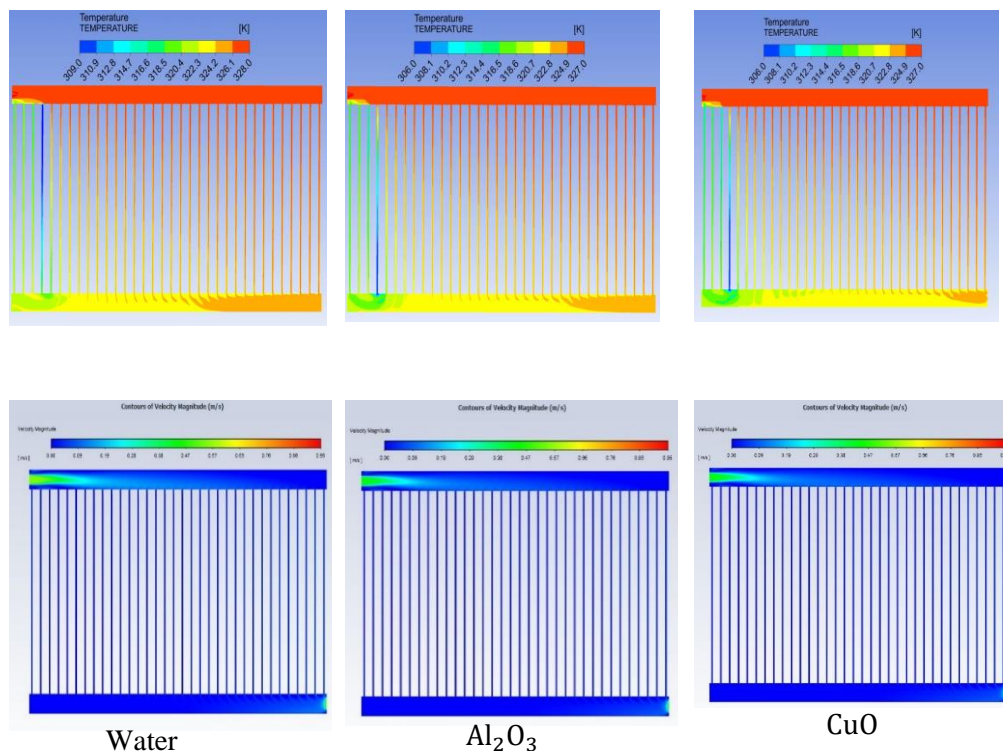


Figure 4.1 Contour plots of water and nanofluids.

The simulations are calculated at different flow rates of inlet coolant ranging from  $4 \text{ l}/\text{min}$  to  $8 \text{ l}/\text{min}$ . By increasing the flow rate 4, 5, 6, 7 and  $8 \text{ l}/\text{min}$ , while the air temperature and heat transfer coefficient is same  $303\text{k}$  and  $150 \text{ W}/\text{m}^2\text{k}$  same for all calculations.

In Fig 4.1 the first row of contour plots representing the temperature distribution at radiator. The first figure of row1 represent the temperature distribution when we used the water as a coolant the 2<sup>nd</sup> and 3<sup>rd</sup> figures represent the temperature distribution of  $\text{Al}_2\text{O}_3$  and  $\text{CuO}$  nanofluids. In the second row the first figure represents the velocity contours of water. The 2<sup>nd</sup> and 3<sup>rd</sup> figures shows the velocity contours of  $\text{Al}_2\text{O}_3$  and  $\text{CuO}$  of nanofluids. These contours plots are obtained at fixed inlet temperature  $55 \text{ }^\circ\text{C}$  and fixed flow rate  $6 \text{ l}/\text{min}$ .

#### 4.4 Results by using $\text{Al}_2\text{O}_3$ Nanoparticles

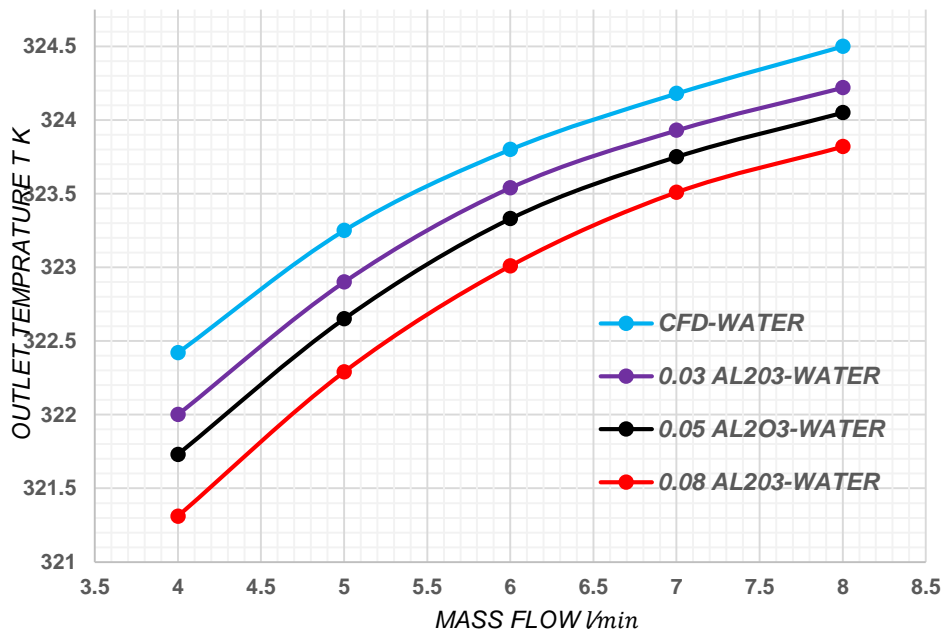


Figure 4.2 Outlet temperature of water and mixture of water and  $\text{Al}_2\text{O}_3$  nanoparticles observed at different mass flow rates.

Fig 4.2 represent the outlet temperature of different radiator coolant at different flow rates. Three different concentrations of  $\text{Al}_2\text{O}_3$  nanoparticles were added

into water. In Fig 4.2 the blue line represents the simulations of water as a coolant, Purple, black and Red lines show the simulations results of nanofluids at different concentration levels of nanoparticles in water. These simulations are carried out at 54 C inlet temperature of radiator coolant. From the graph, it's clear that by increasing the flow rate of coolant the outlet temperature is increase. When we increase the concentration level of nanoparticles in water the outlet temperature of radiator coolant is decrease.

#### 4.5 Results by using *CuO* Nanoparticles

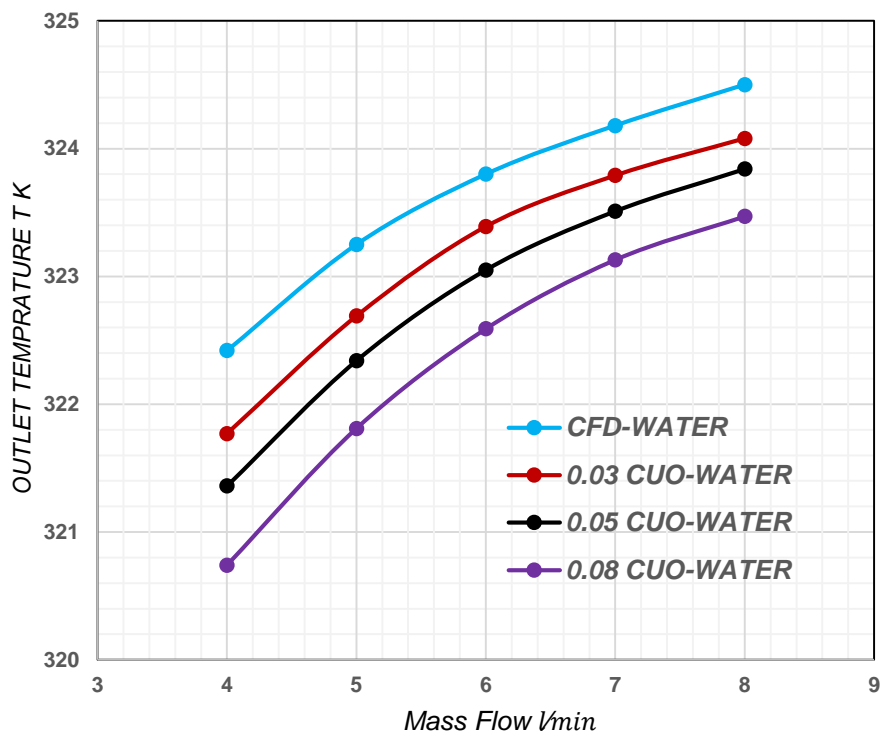


Figure 4.3 Outlet temperature water and mixture of water and *Cuo* nanoparticles observed at different mass flow rates.

Fig 4.3 show the outlet temperature at radiator outlet by using different flow rates of radiator coolant. Three different concentrations of *Cuo* nanoparticles were added into the base fluid(water). In Fig 4.3 Red, black and purple lines represent the simulations results of nanofluids at different concentration levels of *Cuo* nanoparticles in water, while the blue line represents the simulation results of water as a coolant. These simulations results are obtained at 54 °C inlet temperature of inlet coolant. From the graph6, it's clear that by increasing

the flow rate of radiator coolant the outlet temperature of coolant is increase. When we increase the concentration level of  $CuO$  nanoparticles in water the outlet temperature of coolant is decrease. In forced convective boundary conditions, when we compare the graph 5 and 6, the  $CuO$  nanoparticles gives best results as compare to  $Al_2O_3$  nanoparticles in term of outlet temperature.

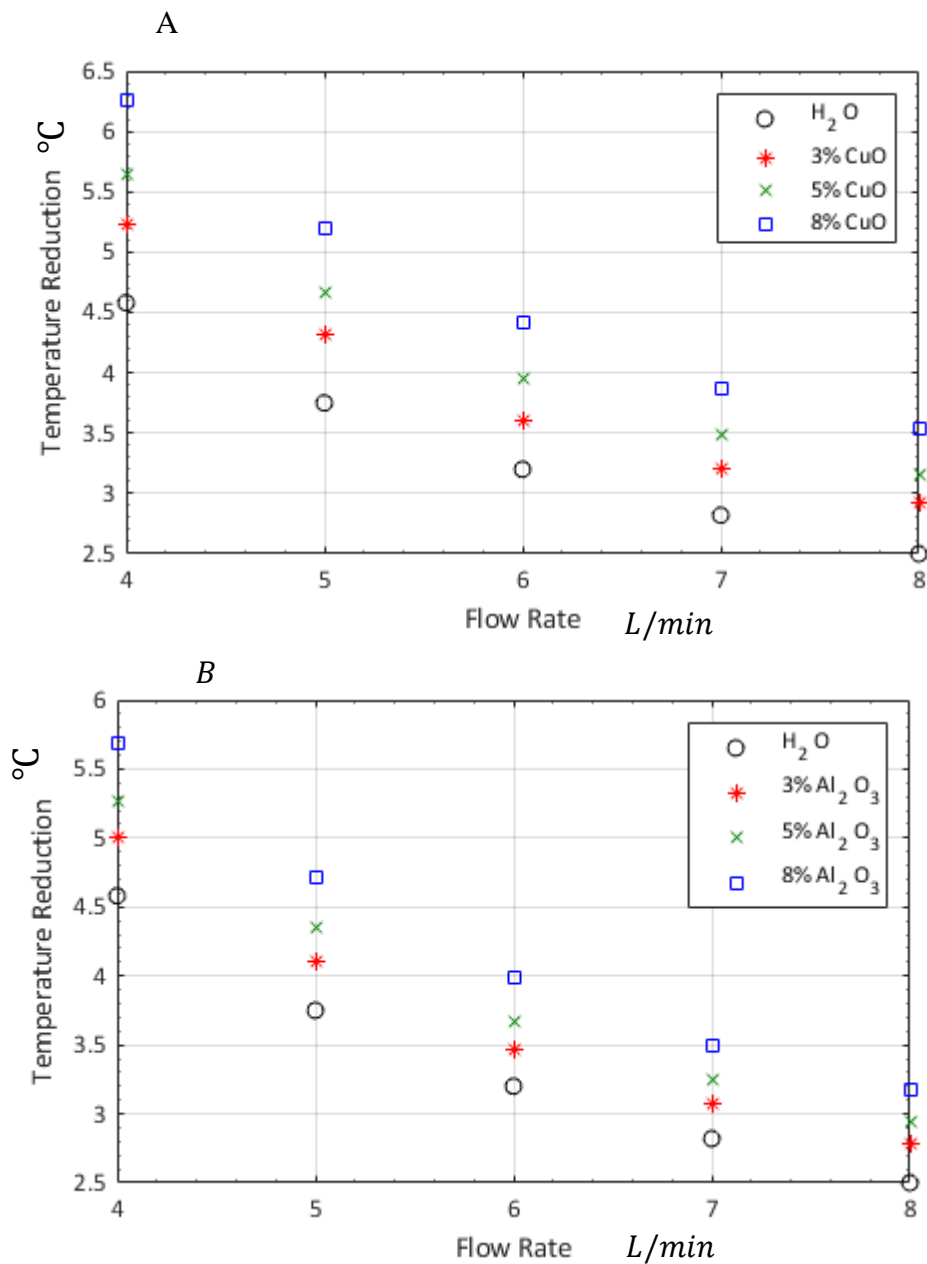


Figure 4.4 A and B Temperature reduction of coolant at different flow rates.

In Fig 4.4 A and B we can see the temperature reduction of different coolants at different flow rates. The temperature reduction of coolant is inversely related to the flow rate when we increase the mass flow rate the temperature reduction is in decreasing order. When the concentration of nanoparticles in base fluid increases the temperature reduction of coolant also increases.

Fig 4.5 show the percentage reduction of outlet temperature when the mass flow rate is changing from 4 to 8  $l/min$ . The percentage temperature reduction is maximum at 0.08 volumetric concentration  $C_{uo}$  nanoparticles in water when the mass flow rate is 4  $l/min$ .

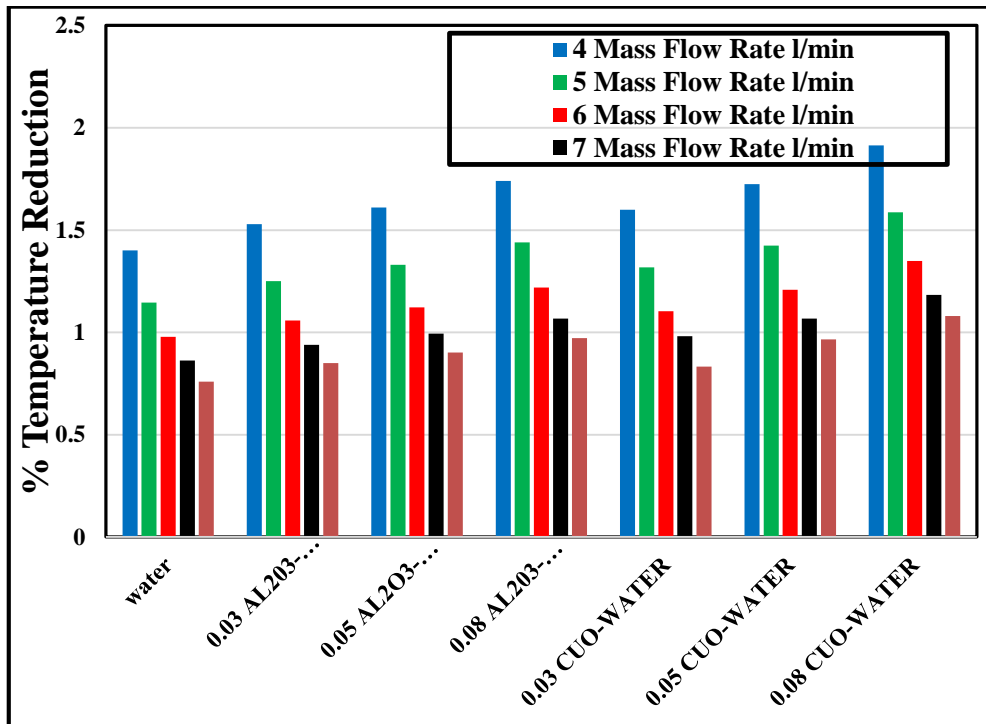


Figure 4.5 Percentage temperature reduction of outlet temperature.

## 4.6 Concluding Remarks

The following are the conclusions of chapter 4.

- i. The outlet temperature of coolant increases by increasing the flow rate.
- ii. When we add the nanoparticles in base fluid, the heat transfer coefficient increases.
- iii. With the increase in volume metric concentration of nanoparticles in base fluid the outlet temperature of coolant is decrease its means that the heat transfer coefficient is increase.
- iv. From the simulations results it's clear that, the *Cuo* nanoparticles in base fluid give minimum outlet temperature at fixed heat transfer coefficient as compare to  $Al_2O_3$  nanoparticles.
- v. The temperature reduction is 1.4% for water.
- vi. The temperature reduction is 1.61% and 1.72% for  $Al_2O_3$  and *CuO* based nanofluids when the nanoparticle concentration is 5%.
- vii. We achieved the maximum temperature reduction of coolant at 0.08 volumetric concentration of *Cuo* in water.
- viii. The percentage temperature reduction is 24.9% for  $Al_2O_3$ -WATER nanofluids.
- ix. The percentage temperature reduction is 36.7% for *CuO* -WATER nanofluids.



### Summary and Future Recommendations

#### 5.1 Summary

In this research we have successfully validated radiator working principle with available literature. The key findings of our work are as follows:

- i. When we increase the mass flow rate the outlet temperature of the radiator increased.
- ii. We achieved the maximum temperature reduction for water is 5.8°C when the inlet temperature of coolant is fixed at 60°C.
- iii. The temperature reduction is 1.4% for water and it is 1.61% and 1.72% for  $\text{Al}_2\text{O}_3$  and  $\text{CuO}$  based nanofluids when the nanoparticle concentration is 5%.
- iv.  $\text{CuO}$  nanoparticles performed better under forced convective boundary conditions as compared to  $\text{Al}_2\text{O}_3$  nanoparticles.
- v. We achieved the maximum temperature reduction 36.7% for  $\text{CuO}$  - WATER nanofluids with 8% volumetric concentration of  $\text{CuO}$  in water.
- vi. However, concentration of nanoparticles above 5% is not recommended as it results in a nonhomogeneous solution and particles agglomeration.

#### 5.2 Future Recommendations

In future, we can expand the present work in the following directions:

- i. We may estimate the natural convective boundary conditions by adding the 3d fan zone and fins in geometry.
- ii. With the use of nanofluids, we may decrease the size of automobile radiators.

## REFERENCES

- [1] Saunders, L. P. (1936). Radiator development and car cooling. *SAE Transactions*, 496-516.
- [2] Müller, R., Rieck, U., Köppl, A., & Stramaccioni, D. (1993). Design and Test of a Honeycomb Radiator Panel with Carbon Fiber Reinforced Plastic Facesheets and Aluminium Heat Pipes. *SAE Transactions*, 1680-1688.
- [3] Okhiria, P. O., & Towoju, O. A.(2021) Design and Analysis of an Automobile Radiator with a 14°C Cooling Capacity. *International Journal of Scientific Research and Engineering Development*— 4 (5)
- [4] Ventola, L., Robotti, F., Dialameh, M., Calignano, F., Manfredi, D., Chiavazzo, E., & Asinari, P. (2014). Rough surfaces with enhanced heat transfer for electronics cooling by direct metal laser sintering. *International Journal of Heat and Mass Transfer*, 75, 58-74.
- [5] Choi, S. U. (2009). Nanofluids: from vision to reality through research. *Journal of Heat transfer*, 131(3).
- [6] Kaufui, V. W., & Omar, D. L. (2010). Applications of nanofluids: Current and future. *Adv. Mech. Eng*, 11, 105-132.
- [7] Routbort, J. (2009). Argonne National Lab, Michellin North America, St. Gobain Corp.
- [8] Ma, H. B., Wilson, C., Borgmeyer, B., Park, K., Yu, Q., Choi, S. U. S., & Tirumala, M. (2006). Effect of nanofluid on the heat transport capability in an oscillating heat pipe. *Applied Physics Letters*, 88(14), 143116.

- [9] Ma, H. B., Wilson, C., Yu, Q., Park, K., Choi, U. S., & Tirumala, M. (2006). An experimental investigation of heat transport capability in a nanofluid oscillating heat pipe.
- [10] Choi, S. U., & Eastman, J. A. (1995). *Enhancing thermal conductivity of fluids with nanoparticles* (No. ANL/MSD/CP-84938; CONF-951135-29). Argonne National Lab.(ANL), Argonne, IL (United States).
- [11] Taylor, R., Coulombe, S., Otanicar, T., Phelan, P., Gunawan, A., Lv, W., ... & Tyagi, H. (2013). Small particles, big impacts: A review of the diverse applications of nanofluids. *Journal of applied physics*, *113*(1), 1.
- [12] Peyghambarzadeh, S. M., Hashemabadi, S. H., Jamnani, M. S., & Hoseini, S. M. (2011). Improving the cooling performance of automobile radiator with Al<sub>2</sub>O<sub>3</sub>/water nanofluid. *Applied thermal engineering*, *31*(10), 1833-1838.
- [13] Khan, T. A., & Ahmad, H. (2019). CFD-based comparative performance analysis of different nanofluids used in automobile radiators. *Arabian Journal for Science and Engineering*, *44*(6), 5787-5799.
- [14] Delavari, V., & Hashemabadi, S. H. (2014). CFD simulation of heat transfer enhancement of Al<sub>2</sub>O<sub>3</sub>/water and Al<sub>2</sub>O<sub>3</sub>/ethylene glycol nanofluids in a car radiator. *Applied thermal engineering*, *73*(1), 380-390.
- [15] Elsebay, M., Elbadawy, I., Shedid, M. H., & Fatouh, M. (2016). Numerical resizing study of Al<sub>2</sub>O<sub>3</sub> and CuO nanofluids in the flat tubes of a radiator. *Applied Mathematical Modelling*, *40*(13-14), 6437-6450.
- [16] Elbadawy, I., Elsebay, M., Shedid, M., & Fatouh, M. (2018). Reliability of nanofluid concentration on the heat transfer augmentation in engine radiator. *International Journal of Automotive Technology*, *19*(2), 233-243.
- [17] Peyghambarzadeh, S. M., Hashemabadi, S. H., Hoseini, S. M., & Jamnani, M. S. (2011). Experimental study of heat transfer enhancement using water/ethylene glycol based nanofluids as a new coolant for car

radiators. *International communications in heat and mass transfer*, 38(9), 1283-1290.

[18] Anoop, K. B., Sundararajan, T., & Das, S. K. (2009). Effect of particle size on the convective heat transfer in nanofluid in the developing region. *International journal of heat and mass transfer*, 52(9-10), 2189-2195.

[19] Moraveji, M. K., Darabi, M., Haddad, S. M. H., & Davarnejad, R. (2011). Modeling of convective heat transfer of a nanofluid in the developing region of tube flow with computational fluid dynamics. *International communications in heat and mass transfer*, 38(9), 1291-1295.

[20] Heris, S. Z., Shokrgozar, M., Poorpharhang, S., Shanbedi, M., & Noie, S. H. (2014). Experimental study of heat transfer of a car radiator with CuO/ethylene glycol-water as a coolant. *Journal of dispersion science and technology*, 35(5), 677-684.

[21] Parashurama, M. S., Dhananjaya, D. A., & Naveena Kumar, R. R. (2015). Experimental study of heat transfer in a radiator using nanofluid. *International Journal of Engineering Development and Research*, 3(2), 307.

[22] Zubair, M. M., Seraj, M., Faizan, M., Anas, M., & Yahya, S. M. (2021). Experimental study on heat transfer of an engine radiator with TiO<sub>2</sub>/EG-water nano-coolant. *SN Applied Sciences*, 3(4), 1-9.

[23] Lelea, D. (2011). The performance evaluation of Al<sub>2</sub>O<sub>3</sub>/water nanofluid flow and heat transfer in microchannel heat sink. *International Journal of Heat and Mass Transfer*, 54(17-18), 3891-3899.

[24] Vajjha, R. S., Das, D. K., & Kulkarni, D. P. (2010). Development of new correlations for convective heat transfer and friction factor in turbulent regime for nanofluids. *International journal of heat and mass transfer*, 53(21-22), 4607-4618.

[25] Fatahian, H., Salarian, H., Nimvari, M. E., & Fatahian, E. (2018). Numerical study of thermal characteristics of fuel oil-alumina and water-alumina nanofluids flow in a channel in the laminar flow. *IIUM Engineering Journal*, 19(1), 251-269.

- [26] Sharma, K. V., Sundar, L. S., & Sarma, P. K. (2009). Estimation of heat transfer coefficient and friction factor in the transition flow with low volume concentration of Al<sub>2</sub>O<sub>3</sub> nanofluid flowing in a circular tube and with twisted tape insert. *International Communications in Heat and Mass Transfer*, 36(5), 503-507.
- [27] Duangthongsuk, W., & Wongwises, S. (2008). Effect of thermophysical properties models on the predicting of the convective heat transfer coefficient for low concentration nanofluid. *International Communications in Heat and Mass Transfer*, 35(10), 1320-1326.
- [28] Duangthongsuk, W., & Wongwises, S. (2008). Effect of thermophysical properties models on the predicting of the convective heat transfer coefficient for low concentration nanofluid. *International Communications in Heat and Mass Transfer*, 35(10), 1320-1326.
- [29] Naraki, M., Peyghambarzadeh, S. M., Hashemabadi, S. H., & Vermahmoudi, Y. (2013). Parametric study of overall heat transfer coefficient of CuO/water nanofluids in a car radiator. *International Journal of Thermal Sciences*, 66, 82-90.
- [30] Tran, N., & Wang, C. C. (2019). Effects of tube shapes on the performance of recuperative and regenerative heat exchangers. *Energy*, 169, 1-17.
- [31] Young, D. F., Munson, B. R., Okiishi, T. H., & Huebsch, W. W. (2010). *A brief introduction to fluid mechanics*. John Wiley & Sons.
- [32] Potter, M. C., & Wiggert, D. C. (2021). *Schaum's Outline of Fluid Mechanics*. McGraw-Hill Education.
- [33] Dusenbery, D. B. (2009). *Living at micro scale: the unexpected physics of being small*. Harvard University Press.
- [34] Versteeg, H. K., & Malalasekera, W. (2007). *An introduction to computational fluid dynamics: the finite volume method*. Pearson education.

[35] Çengel, Y. A., & Ghajar, A. J. (2002). Heat conduction equation. *Heat Transfer A Practical Approach, 2nd ed. McGraw-Hill Higher Education*, 61-126.

[36] Chiavazzo, E., Ventola, L., Calignano, F., Manfredi, D., & Asinari, P. (2014). A sensor for direct measurement of small convective heat fluxes: Validation and application to micro-structured surfaces. *Experimental Thermal and Fluid Science*, 55, 42-53.